Cell Tissue Res
DOI 10.1007/s00441-007-0546-8

REVIEW

Stem cells and neonatal brain injury

Tomoaki Ikeda

Received: 22 August 2007 / Accepted: 25 October 2007

Abstract Recent advances in regenerative medicine and in our understanding of neurogenesis may lead to new ways of recovering neuronal function lost or damaged during the perinatal period; such injuries are not amenable to conventional therapies. We review recent experimental studies based on immature rodents models of neonatal brain injury, especially hypoxic-ischemic encephalopathy. The developing brain is revealed to have considerable potential with respect to proliferation and migration to the injured site. However, the generation of fully differentiated neurons is extremely limited after brain injuries. Aggressive efforts to adjust the environment of the damaged brain in which tissue regeneration is occurring or more cautious stem cell transplantation will be required for the successful treatment of developmental brain injury.

Keywords Neonatal brain injury · Hypoxia-ischemia · Neural stem/progenitor cell

Introduction

Neonatal brain injury exhibits some unique aspects that are not seen in adult brain damage. The abnormal symptoms and signs characterizing neonatal brain injury are thought to be mainly associated with adverse events that happen in the antenatal period (Badawi et al. 1998a, 1998b). Amongst the precipitating events are trauma, metabolic abnormalities, infection, hypoxia, ischemia, and the presence of toxins (Volpe 2000). Another factor is that antenatal brain injuries are rarely diagnosed in the neonatal period but instead are discovered later in life and are diagnosed as, for example, cerebral palsy, mental retardation, epilepsy, cognitive disturbances, and learning disability (van de Riet 1999). Relatively minor brain injuries received during the perinatal period can also evolve into variable functional impairments as infants grow (Mishima et al. 2005).

Clearly, therapeutic modalities are not easy to perform just after an insult occurs during the perinatal period. This is especially true in the fetal brain. With regard to hypoxic-ischemic encephalopathy, which accounts for about 10% of neonatal brain injuries (Hankins and Speer 2003), the intensive monitoring of intrapartum fetal well-being together with fetal heart rate patterns (Parer and Ikeda 2007), the application of an adequate neonatal resuscitation program, and hypothermic treatment for moderately affected infants (Gluckman et al. 2006), all seem to have a beneficial impact on the outcome of hypoxic-ischemic-induced brain injury. However, to date, no definitive evidence has been provided on the possible decrease in cerebral palsy or other developmental brain disorders.

Once brain damage is established, the resulting chronically injured status dose not seem to be amenable to conventional therapies. Thus, regenerative therapies, cell transplantation, and gene therapy have been proposed as possible methods to overcome long-lasting devastating disorders. Recent advances in regenerative medicine and in our understanding of neurogenesis may lead to ways of recovering neuronal functions that may be lost in perinatal

This work was supported by a Research Grant for Cardiovascular Diseases (18C-1) from the Ministry of Health, Labour and Welfare.

T. Ikeda
Department of Perinatology, National Cardiovascular Center, Osaka, Japan

T. Ikeda (✉)
25-7-1 Fujishiro-dai, Suita,
Osaka 565-8565, Japan
e-mail: tikeda44@hotmail.com

brain injury. In this paper, we describe recent experimental results, including data from our laboratory, regarding neuronal stem cell and neonatal brain damage. We have limited this review to hypoxic-ischemic brain injury as a model of disorder in neonatal brain injury, because it has been most investigated and is the best described (Park et al. 2002a).

Endogenous stem cell proliferation in response to hypoxic-ischemic injury

The immature and developing brain might be expected to possess a more potent capacity with respect to neurogenesis and plasticity compared with the adult brain. Neurogenesis comprises cell proliferation, migration, and differentiation (Iwai et al. 2002, 2003). We have carried out a series of experiments to elucidate endogenous behavior, in terms of these factors, in the immature rat brain in response to a unilateral hypoxic-ischemic insult (Hayashi et al. 2005; Ikeda et al. 2005; Iwai et al. 2006). For these studies, we used the Rice-Vannucci rat model in which a 2-h period of hypoxia was imposed after ligation of the left carotid artery. This choice of model was based on its wide use in neonatal hypoxic-ischemic encephalopathy (Vannucci 1990). The contralateral (non-ligated) brain hemisphere acts as a control for hypoxic stress, in addition to non-hypoxic-ischemic sham controls. The stable survival of the treated rats is also an advantage in this model, because long-term effects can be readily evaluated (Hagberg et al. 2002).

In order to assess the proliferation of neuronal stem cells, bromodeoxyuridine (BrdU), which is incorporated into DNA as a nucleotide base, was used to label the dividing cells. We performed an intraperitoneal injection of single-dose BrdU (50 mg/kg) on postnatal day 7 (P7) in the basal group and on 1 day (P8), 7 days (P14), 14 days (P21), and 21 days (P28) after hypoxia-ischemia. The brain was retrieved 2 h after BrdU injection. When immunoreactive BrdU-positive cells were counted in the subventricular zone (SVZ) of the lateral ventricle (the most important germinal matrix of the rat), the number of BrdU-labeled cells in the injured (left) side of the hypoxic-ischemic brain was twice the level of that in the sham controls at 7 days after hypoxia-ischemia. Interestingly, the non-injured (right) side of the hypoxic-ischemic brain showed a comparable number of BrdU-positive cells to the injured side (Fig. 1). Both sides returned to the control level by 21 days after hypoxia-ischemia.

The finding that a unilateral hypoxic-ischemic insult enhanced neural stem cell proliferation, not only in the injured brain, but also on the other uninjured side indicates that humoral factors might influence proliferation both. This supposition is supported by recent experiments (Park et al. 2006a) in which a soluble fraction and a membrane fraction have been extracted from hypoxic-ischemic neonate brain hemispheres, in acute and chronic stages; the extracts significantly facilitate mitosis of a neuronal stem cell line in vitro.

Our results are consistent with previous reports of increased proliferation and neurogenesis in the SVZ region after hypoxic-ischemic stress in neonatal rodents (Ong et al. 2005; Park et al. 2006a; Plane et al. 2004; Qiu et al. 2007; Yang and Levison 2006). Although increased proliferation has been seen in both SVZs (injured/non-injured), the phenotype of the proliferating cells appears to be significantly different. Levison and colleagues (Felling et al. 2006; Yang and Levison 2006) have harvested SVZ from both sides of neonatal rats at 48 h of recovery and have cultured the cells in vitro as neurospheres in the presence of the fibroblast growth factor (FGF-2) and epidermal growth factor (EGF). When the neurospheres are further differentiated in growth-factor-free medium for 5 days, injured-side-derived neurospheres are significantly larger than those from the non-injured side or from a sham-control and have more cells showing tripotential neural stem/progenitor cell markers such as nestin, Notch1, and EGF-receptor. Injured-side-derived neurospheres also differentiate preferentially into oligodendrocytes and neuronal cells than into astroglia. These findings indicate that, in the injured side, increased proliferation within the neuronal stem/progenitor cell lineage occurs 2 days after hypoxia-ischemia. We speculate that this effect compensates for the vulnerability in neurons and oligodendrocytes in the developmental stage (Back et al. 2001, 2002).

Endogenous stem cell migration following hypoxic-ischemic injury

Doublecortine (DCX) is a marker for migrating neuronal precursor cells, the early stage of neuronal differentiation from multipotent neuronal stem cells (Francis et al. 1999; Gleeson et al. 1999). We have used an anti-DCX antibody to evaluate the migrating activity of the precursor. Rat brains were retrieved 7 (P14), 14 (P21), and 21 (P28) days after hypoxic-ischemic insult on postnatal day 7. Each rat was administered BrdU (50 mg/kg, six times, 12 h apart) for the last 3 days before brain retrieval. At 7 days after hypoxia-ischemia, 456±72 BrdU-positive cells/mm^2 were found around the cortical infarcted area, with 24% of BrdU-positive cells being DCX positive. By contrast, there were only 88 and 106 BrdU-positive cells in the corresponding areas of uninjured cortex and sham-control cortex, respectively. Moreover, in control cortices, few cells (only 0.6% of the BrdU-positive cells each) were positive for DCX. The total number of BrdU-positive cells in the infarcted cortex decreased gradually 14 and 21 days after hypoxia-

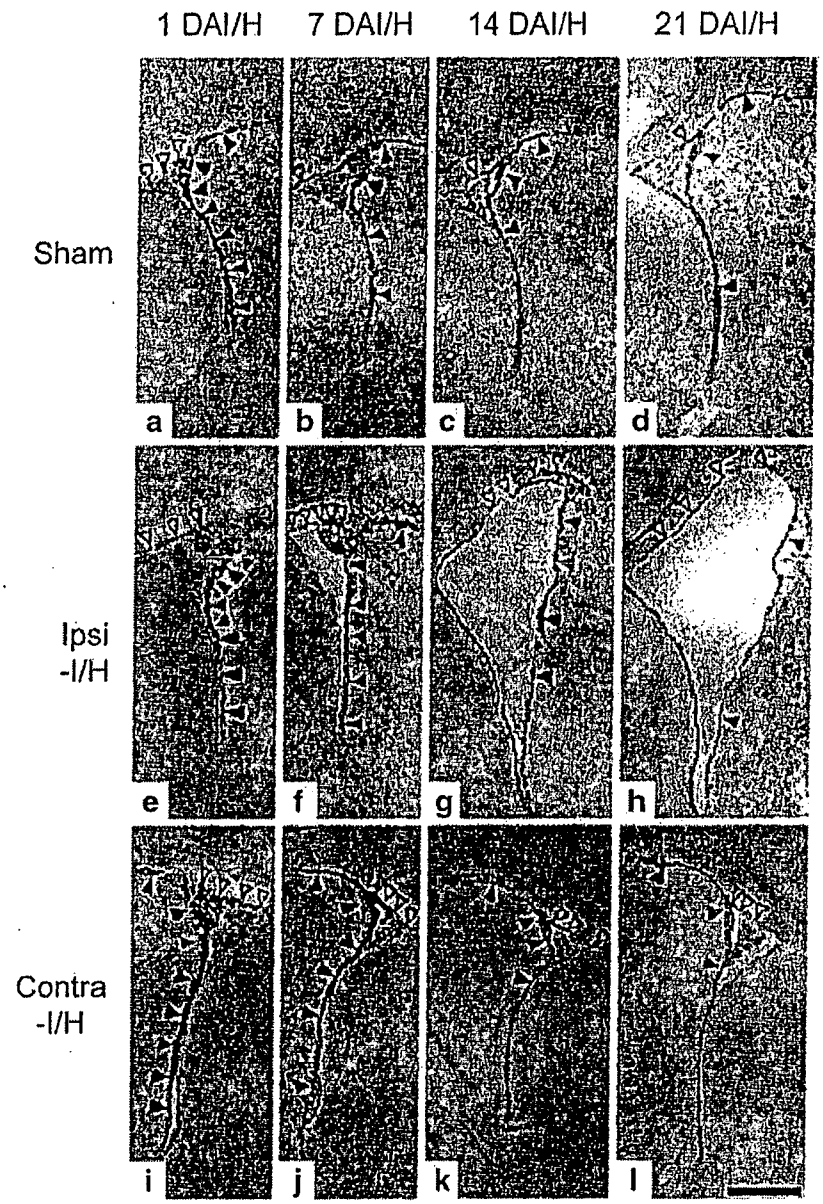

Fig. 1 Immunohistochemical staining for bromodeoxyuridine (BrdU) in the subventricular zone (SVZ) of sham-control animals (*Sham*, **a–d**), the ipsilateral side of ischemia/hypoxia brain (*Ipsi-I/H*, **e–h**), and the contralateral side of ischemia/hypoxia brain (*Contra-I/H*, **i–l**), 1 day (*1 DAI/H*, **a**, **e**, **i**), 7 days (*7 DAI/H*, **b**, **f**, **j**), 14 days (*14 DAI/H*, **c**, **g**, **k**), and 21 days (*21 DAI/H*, **d**, **h**, **l**) after insult. In SVZa, which lines the lateral wall of the lateral ventricle (LV), in both *Ipsi-I/H* and *Contra-I/H* brains, large numbers of BrdU-labeled cells (*black arrowheads*) were detected from 1 to 7 days after insult compared with the sham control. Note that, in SVZb, which lines the upper wall of the LV, in both *Ipsi-I/H* and *Contra-I/H* brains, large numbers of BrdU-labeled cells (*open arrowheads*) could be detected from 7 to 21 days after insult compared with the sham control. Data were derived from Iwai et al. (2006)

ischemia, whereas the percentage of DCX-positive cells remained constant at around 25%. This finding of a significant migration of DCX-positive newly divided cells around the infarction area, but not on the non-injured side, is consistent with other experiments on neonatal rats or mice (Felling et al. 2006; Yang and Levison 2006). The rate of migration in the neonatal brain seems to be greater than that in the adult brain (Jin et al. 2001; Zhang et al. 2001), indicating the powerful regenerative potential of the neonatal brain.

Several candidate chemotaxic factors have been proposed to attract neuronal progenitor cells. Quantitative polymerase chain reaction of the isolated brain from neonatal rats allowed to recover for 3 and 14 days after hypoxia-ischemic treatment showed that monocyte chemoattractant protein-1 (MCP-1) significantly increased in the

cortex, and that its receptor, CCR-2, also increased in the SVZ and cortex (Yang et al. 2007). Stromal derived factor-1 (SDF-1) and its receptor CXCR-4 are other potential candidate chemotaxic factors (Miller et al. 2005).

One important question is whether a neural stem cell proliferating in the SVZ of the non-injured side migrates into the injured side to take part in regeneration. In recent experiments, Park et al. (2006a) clearly demonstrated that this can occur through the corpus collosum and fimbria. In this study, they injected the clonal multipotent neural precursor cell line (C17.2) derived from the external germinal layer of the neonatal mouse cerebellum and incorporating the lacZ-expressing molecule as a reporter marker into neonatal rat brain; the engrafted C17.2 cells migrated from the non-injured hemisphere to the injured side.

Endogenous stem cell differentiation after hypoxic-ischemic injury

Previously, we have used an anti-neuronal nuclear antigen (NeuN) antibody to detect matured neurons, together with BrdU, as an early marker of cell proliferation (Ikeda et al. 2005). BrdU was administrated at days 5–7 (50 mg/kg intraperitoneally, six times, in total) after hypoxia-ischemia on postnatal day 7, and rat brains were extracted 14 (P21), 28 (P35), and 42 days (P49) later. At 14 days after hypoxia-ischemia, 121 BrdU-positive cells/mm^2 were found around the injured cavity. Unexpectedly, and rather disappointingly, only 1% of BrdU-positive cells were mature neurons (NeuN-immunopositive; Fig. 2). BrdU-positive cells represented cells that would have divided 7–9 days previously (i.e., 5–7 days after the hypoxic-ischemic insult), when the cells would have been undergoing maximum proliferation in the SVZ. This cohort of cells must have migrated to the infarcted area in the cortex at 7 days after hypoxia-ischemia.

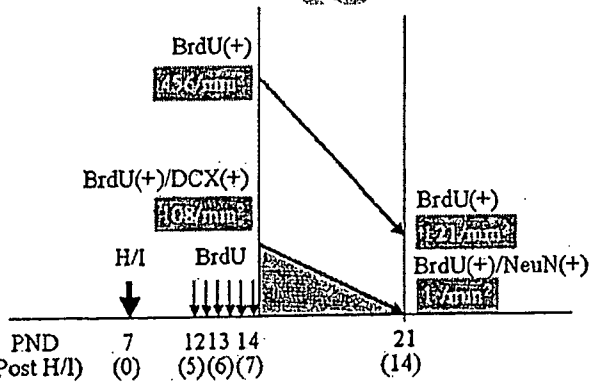

Fig. 2 Schematic explanation of the limited differentiation from neural progenitor cells that are doubly immunopositive for BrdU and doublecortine (*DCX*) to mature neurons positive for BrdU and neuronal nuclear antigen (*NeuN*). At 7 days after hypoxic-ischemic (*H/I*) treatment, 108 of 456 BrdU-positive cells that were around the infarcted area were immunopositive for DCX. At 14 days after H/I treatment, however, only a single cell differentiated into a mature neuron out of 108 migrating neural progenitor cells (*PND* postnatal day). Data derived from Ikeda et al. (Ikeda et al. 2005)

Few newly formed neurons could be found no more than 28 days after the hypoxic-ischemic insult. This finding is consistent with the observation by Morshead and van der Kooy (1992) that most newly generated neurons in the adult appear to undergo programmed cell death, rather than surviving to make a neuronal network. Furthermore, the nuclear morphology of the cells doubly immunopositive for BrdU and NeuN suggests that they were "interneurons", rather than pyramidal neurons, as observed by Yang et al. (2007). These newly recruited neurons are apparently ineligible to connect with other neurons to make a neural network or to contribute, even partially, to functional recovery. This significantly impaired ability to differentiate contrasts with the successful differentiation into neurons and astroglia of externally injected human neural stem cells, in experiments with normally developing animal brains (Ourednik et al. 2001). Our data may be explained by the poor environment provided by the infarcted cortex. There may be poor neural inputs and outputs or a poor humoral milieu (such as low levels of neurotrophic factors). The reduced self-repairing ability in this model seems to be related to the large area of cell degeneration. Daval et al. (2004) have reported complete self-repair in the hippocampus region CA1 of neonatal rats. In their study, transient hypoxia results in merely a small reduction in the neuronal cells in this region. Thus, the hypoxic-ischemic insult in the present study may be too severe for successful neuronal self-repair.

The finding of the severely limited ability to differentiate from neuronal precursor cells to mature neurons implies that attempts to produce functional recovery by simple stem cell transplantation is unlikely to an effective method of treating neonatal hypoxic-ischemic encephalopathy.

Neuroregeneration in neonatal hippocampus

Fewer studies of the neuroregeneration of other areas have been reported compared with those of the neonatal brain cortex. The complete self-repair of damage in the CA1 region of the hippocampus in the study of Daval et al. (2004; see also above) may be alternatively explained by the regional difference of the neonatal brain. Recently, Qiu et al. (2007) have studied endogenous proliferation and differentiation after hypoxia-ischemia in neonate (postnatal day 9) and juvenile (postnatal day 21) mouse. Contrary to what has been generally assumed, their results indicate that the juvenile brain has a greater capacity for neurogenesis

after injury than the immature neonatal brain. In addition to regional differences, we should thus consider developmental age when trying to apply a regenerative therapy to developing brain.

Transplantation of neural stem cells

Zheng et al. (2006) extracted multipotent astrocytic stem cells from the subependymal zones of homozygous green fluorescence protein (GFP) transgenic neonatal mice at postnatal days 1–6. These cells are positive for glial fibrillary acidic protein and negative for beta-III tubulin and NeuN, markers of mature neurons (Laywell et al. 2000). The multipotent astrocytic stem cells were transplanted into Sprague-Dawley rat brains 24 h or 5 days after hypoxia-ischemia on postnatal day 7 (Zheng et al. (2006). GFP-positive cells successfully transformed into neurons positive for beta-III tubulin and NeuN and were located around the infarcted area, far from the injection site. This observation was however not quantitative, and furthermore, the authors did not describe any histological or behavioral improvements.

In a study by Park et al (2002b), the clonal multipotent neural precursor cell line (C17.2) was derived from the external germinal layer of the neonatal mouse cerebellum; these neural stem/progenitor cells were cultured with a polymer scaffold (polyglycolic acid, PGA), for 4 days, making a neural stem/progenitor cell-PGA complex. The neural stem/progenitor cell-PGA matrix was transplanted into the degenerated cavity of mouse brain, 7 days after hypoxia-ischemia on postnatal day 7. The transplanted neural stem cells not only differentiated into neurons, oligodendrocytes, and astrocytes, but also made neural networks with both donor-derived neurons and host-derived neurons. This neuronal network extended through the corpus callosum into the contralateral hemisphere. Although Park et al (2002b) reported that neurological function, as assessed by diminished unilateral rotation, seemed to be improved, they did not quantitatively analyze behavioral improvement.

Exogenous enrichment of the milieu around the injury

Another way to facilitate regeneration may be the enrichment of the milieu around the injured region. Neurotrophic factors play an important role in the development and maintenance of specific populations of neurons in the central and peripheral nervous system. Several neurotrophic factors have been reported to help rescue neurons and repair neuronal injury. These include nerve growth factor (NGF), brain-derived neurotrophic factor (BDNF), glial-cell line-derived neurotrophic factor (GDNF), insulin-like growth factor, basic fibroblast growth factor (bFGF), transforming growth factor (TGF)-beta 3, neurotrophin-3 (NT-3), NT-4/5, and NT-6 (Gong et al. 1999; Hyman et al. 1994; Ikeda et al. 2000; Krieglstein et al. 1996; Zawada et al. 1998). Although these neurotrophic factors are also known to be upregulated after hypoxia-ischemia in the neonatal rat (Ikeda et al. 2002), this endogenous upregulation seems to be insufficient to support neural differentiation from progenitor cells.

To date, bFGF-2 seems to be the most promising candidate to facilitate neuroregeneration in neonatal bran damage (Wagner et al. 1999). Monfils et al. (2006, 2005) administered 50 ng/kg bFGF for 7 days after brain lesions to the motor cortex of a neonatal rat and observed significant neuronal recovery and synapse formation in the treated group. This was accompanied with improved forelimb movement. Although this injury is traumatic, bFGF could be applied after hypoxic-ischemic injury with or without another neurotrophic factor such ase EGF (Nakatomi et al. 2002).

Recently, Park et al. (2006b) transplanted a subclone of neural stem cells, transduced with a retrovirus encoding NT-3, into a site of unilateral hypoxic-ischemic brain damage in neonatal mice. They observed a greater than 80% increase in neurons derived from neural stem cells compared with those from non-transduced stem cells. Donor-derived stem cells were shown to differentiate successfully into cholinergic, gamma-aminobuytric-acidergic, or glutamatergic subtypes of neuron. These findings indicate the importance of adjusting the environment around the injured area for successful stem cell therapy.

Concluding remarks

Although considerable potential with respect to proliferation and migration has been revealed in the immature and developing brain, limitated terminal differentiation may hamper stem cell therapy. Aggressive efforts to adjust the environment of the damaged part in which tissue regeneration is occurring or more cautious stem cell transplantation will probably be required.

Acknowledgement I thank Professor Dr. Alistair J. Gunn, Professor of the Liggins Institute and Department of Paediatrics, New Zealand, for expert suggestions and proofreading.

References

Back SA, Luo NL, Borenstein NS, Levine JM, Volpe JJ, Kinney HC (2001) Late oligodendrocyte progenitors coincide with the developmental window of vulnerability for human perinatal white matter injury. J Neurosci 21:1302–1312

Back SA, Han BH, Luo NL, Chricton CA, Xanthoudakis S, Tam J, Arvin KL, Holtzman DM (2002) Selective vulnerability of late oligodendrocyte progenitors to hypoxia-ischemia. J Neurosci 22:455–463

Badawi N, Kurinczuk JJ, Keogh JM, Alessandri LM, O'Sullivan F, Burton PR, Pemberton PJ, Stanley FJ (1998a) Antepartum risk factors for newborn encephalopathy: the Western Australian case-control study. BMJ 317:1549–1553

Badawi N, Kurinczuk JJ, Keogh JM, Alessandri LM, O'Sullivan F, Burton PR, Pemberton PJ, Stanley FJ (1998b) Intrapartum risk factors for newborn encephalopathy: the Western Australian case-control study. BMJ 317:1554–1558

Daval JL, Pourie G, Grojean S, Lievre V, Strazielle C, Blaise S, Vert P (2004) Neonatal hypoxia triggers transient apoptosis followed by neurogenesis in the rat CA1 hippocampus. Pediatr Res 55:561–567

Felling RJ, Snyder MJ, Romanko MJ, Rothstein RP, Ziegler AN, Yang Z, Givogri MI, Bongarzone ER, Levison SW (2006) Neural stem/progenitor cells participate in the regenerative response to perinatal hypoxia/ischemia. J Neurosci 26:4359–4369

Francis F, Koulakoff A, Boucher D, Chafey P, Schaar B, Vinet MC, Friocourt G, McDonnell N, Reiner O, Kahn A, McConnell SK, Berwald-Netter Y, Denoulet P, Chelly J (1999) Doublecortin is a developmentally regulated, microtubule-associated protein expressed in migrating and differentiating neurons. Neuron 23:247–256

Gleeson JG, Lin PT, Flanagan LA, Walsh CA (1999) Doublecortin is a microtubule-associated protein and is expressed widely by migrating neurons. Neuron 23:257–271

Gluckman PD, Gunn AJ, Wyatt JS (2006) Hypothermia for neonates with hypoxic-ischemic encephalopathy. N Engl J Med 354:1643–1645

Gong L, Wyatt RJ, Baker I, Masserano JM (1999) Brain-derived and glial cell line-derived neurotrophic factors protect a catecholaminergic cell line from dopamine-induced cell death. Neurosci Lett 263:153–156

Hagberg H, Ichord R, Palmer C, Yager JY, Vannucci SJ (2002) Animal models of developmental brain injury: relevance to human disease. A summary of the panel discussion from the Third Hershey Conference on Developmental Cerebral Blood Flow and Metabolism. Dev Neurosci 24:364–366

Hankins GD, Speer M (2003) Defining the pathogenesis and pathophysiology of neonatal encephalopathy and cerebral palsy. Obstet Gynecol 102:628–636

Hayashi T, Iwai M, Ikeda T, Jin G, Deguchi K, Nagotani S, Zhang H, Sehara Y, Nagano I, Shoji M, Ikenoue T, Abe K (2005) Neural precursor cells division and migration in neonatal rat brain after ischemic/hypoxic injury. Brain Res 1038:41–49

Hyman C, Juhasz M, Jackson C, Wright P, Ip NY, Lindsay RM (1994) Overlapping and distinct actions of the neurotrophins BDNF, NT-3, and NT-4/5 on cultured dopaminergic and GABAergic neurons of the ventral mesencephalon. J Neurosci 14:335–347

Ikeda T, Xia XY, Xia YX, Ikenoue T, Han B, Choi BH (2000) Glial cell line-derived neurotrophic factor protects against ischemia/hypoxia-induced brain injury in neonatal rat. Acta Neuropathol (Berl) 100:161–167

Ikeda T, Koo H, Xia YX, Ikenoue T, Choi BH (2002) Bimodal upregulation of glial cell line-derived neurotrophic factor (GDNF) in the neonatal rat brain following ischemic/hypoxic injury. Int J Dev Neurosci 20:555–562

Ikeda T, Iwai M, Hayashi T, Nagano I, Shogi M, Ikenoue T, Abe K (2005) Limited differentiation to neurons and astroglia from neural stem cells in the cortex and striatum after ischemia/hypoxia in the neonatal rat brain. Am J Obstet Gynecol 193:849–856

Iwai M, Sato K, Omori N, Nagano I, Manabe Y, Shoji M, Abe K (2002) Three steps of neural stem cells development in gerbil dentate gyrus after transient ischemia. J Cereb Blood Flow Metab 22:411–419

Iwai M, Sato K, Kamada H, Omori N, Nagano I, Shoji M, Abe K (2003) Temporal profile of stem cell division, migration, and differentiation from subventricular zone to olfactory bulb after transient forebrain ischemia in gerbils. J Cereb Blood Flow Metab 23:331–341

Iwai M, Ikeda T, Hayashi T, Sato K, Nagata T, Nagano I, Shoji M, Ikenoue T, Abe K (2006) Temporal profile of neural stem cell proliferation in the subventricular zone after ischemia/hypoxia in the neonatal rat brain. Neurol Res 28:461–468

Jin K, Minami M, Lan JQ, Mao XO, Batteur S, Simon RP, Greenberg DA (2001) Neurogenesis in dentate subgranular zone and rostral subventricular zone after focal cerebral ischemia in the rat. Proc Natl Acad Sci USA 98:4710–4715

Krieglstein K, Maysinger D, Unsicker K (1996) The survival response of mesencephalic dopaminergic neurons to the neurotrophins BDNF and NT-4 requires priming with serum: comparison with members of the TGF-beta superfamily and characterization of the serum-free culture system. J Neural Transm Suppl 47:247–258

Laywell ED, Rakic P, Kukekov VG, Holland EC, Steindler DA (2000) Identification of a multipotent astrocytic stem cell in the immature and adult mouse brain. Proc Natl Acad Sci USA 97:13883–13888

Miller JT, Bartley JH, Wimborne HJ, Walker AL, Hess DC, Hill WD, Carroll JE (2005) The neuroblast and angioblast chemotaxic factor SDF-1 (CXCL12) expression is briefly up regulated by reactive astrocytes in brain following neonatal hypoxic-ischemic injury. BMC Neurosci 6:63

Mishima K, Ikeda T, Aoo N, Takai N, Takahashi S, Egashira N, Ikenoue T, Iwasaki K, Fujiwara M (2005) Hypoxia-ischemic insult in neonatal rats induced slowly progressive brain damage related to memory impairment. Neurosci Lett 376:194–199

Monfils MH, Driscoll I, Vandenberg PM, Thomas NJ, Danka D, Kleim JA, Kolb B (2005) Basic fibroblast growth factor stimulates functional recovery after neonatal lesions of motor cortex in rats. Neuroscience 134:1–8

Monfils MH, Driscoll I, Kamitakahara H, Wilson B, Flynn C, Teskey GC, Kleim JA, Kolb B (2006) FGF-2-induced cell proliferation stimulates anatomical, neurophysiological and functional recovery from neonatal motor cortex injury. Eur J Neurosci 24:739–749

Morshead CM, Kooy D van der (1992) Postmitotic death is the fate of constitutively proliferating cells in the subependymal layer of the adult mouse brain. J Neurosci 12:249–256

Nakatomi H, Kuriu T, Okabe S, Yamamoto S, Hatano O, Kawahara N, Tamura A, Kirino T, Nakafuku M (2002) Regeneration of hippocampal pyramidal neurons after ischemic brain injury by recruitment of endogenous neural progenitors. Cell 110:429–441

Ong J, Plane JM, Parent JM, Silverstein FS (2005) Hypoxic-ischemic injury stimulates subventricular zone proliferation and neurogenesis in the neonatal rat. Pediatr Res 58:600–606

Ourednik V, Ourednik J, Flax JD, Zawada WM, Hutt C, Yang C, Park KI, Kim SU, Sidman RL, Freed CR, Snyder EY (2001) Segregation of human neural stem cells in the developing primate forebrain. Science 293:1820–1824

Parer JT, Ikeda T (2007) A framework for standardized management of intrapartum fetal heart rate patterns. Am J Obstet Gynecol 197 (26):e1–e6

Park KI, Ourednik J, Ourednik V, Taylor RM, Aboody KS, Auguste KI, Lachyankar MB, Redmond DE, Snyder EY (2002a) Global gene and cell replacement strategies via stem cells. Gene Ther 9:613–624

Park KI, Teng YD, Snyder EY (2002b) The injured brain interacts reciprocally with neural stem cells supported by scaffolds to reconstitute lost tissue. Nat Biotechnol 20:1111–1117

Park KI, Hack MA, Ourednik J, Yandava B, Flax JD, Stieg PE, Gullans S, Jensen FE, Sidman RL, Ourednik V, Snyder EY (2006a) Acute injury directs the migration, proliferation, and differentiation of solid organ stem cells: evidence from the effect of hypoxia-ischemia in the CNS on clonal "reporter" neural stem cells. Exp Neurol 199:156–178

Park KI, Himes BT, Stieg PE, Tessler A, Fischer I, Snyder EY (2006b) Neural stem cells may be uniquely suited for combined gene therapy and cell replacement: evidence from engraftment of neurotrophin-3-expressing stem cells in hypoxic-ischemic brain injury. Exp Neurol 199:179–190

Plane JM, Liu R, Wang TW, Silverstein FS, Parent JM (2004) Neonatal hypoxic-ischemic injury increases forebrain subventricular zone neurogenesis in the mouse. Neurobiol Dis 16:585–595

Qiu L, Zhu C, Wang X, Xu F, Eriksson PS, Nilsson M, Cooper-Kuhn CM, Kuhn HG, Blomgren K (2007) Less neurogenesis and inflammation in the immature than in the juvenile brain after cerebral hypoxia-ischemia. J Cereb Blood Flow Metab 27:785–794

Riet JE van de, Vandenbussche FP, Le Cessie S, Keirse MJ (1999) Newborn assessment and long-term adverse outcome: a systematic review. Am J Obstet Gynecol 180:1024–1029

Vannucci RC (1990) Experimental biology of cerebral hypoxia-ischemia: relation to perinatal brain damage. Pediatr Res 27:317–326

Volpe JJ (2000) Neurology of the neonate, 4th edn. Saunders, Philadelphia

Wagner JP, Black IB, DiCicco-Bloom E (1999) Stimulation of neonatal and adult brain neurogenesis by subcutaneous injection of basic fibroblast growth factor. J Neurosci 19:6006–6016

Yang Z, Levison SW (2006) Hypoxia/ischemia expands the regenerative capacity of progenitors in the perinatal subventricular zone. Neuroscience 139:555–564

Yang Z, Covey MV, Bitel CL, Ni L, Jonakait GM, Levison SW (2007) Sustained neocortical neurogenesis after neonatal hypoxic/ischemic injury. Ann Neurol 61:199–208

Zawada WM, Zastrow DJ, Clarkson ED, Adams FS, Bell KP, Freed CR (1998) Growth factors improve immediate survival of embryonic dopamine neurons after transplantation into rats. Brain Res 786:96–103

Zhang RL, Zhang ZG, Zhang L, Chopp M (2001) Proliferation and differentiation of progenitor cells in the cortex and the subventricular zone in the adult rat after focal cerebral ischemia. Neuroscience 105:33–41

Zheng T, Rossignol C, Leibovici A, Anderson KJ, Steindler DA, Weiss MD (2006) Transplantation of multipotent astrocytic stem cells into a rat model of neonatal hypoxic-ischemic encephalopathy. Brain Res 1112:99–105

THE JOURNAL OF BIOLOGICAL CHEMISTRY VOL. 282, NO. 35, pp. 25445–25452, August 31, 2007

Role of MAPK Phosphatase-1 in the Induction of Monocyte Chemoattractant Protein-1 during the Course of Adipocyte Hypertrophy*[S]

Received for publication, February 21, 2007, and in revised form, June 14, 2007 Published, JBC Papers in Press, July 3, 2007, DOI 10.1074/jbc.M701549200

Ayaka Ito[‡§1], Takayoshi Suganami[‡], Yoshihiro Miyamoto[¶], Yasunao Yoshimasa[¶], Motohiro Takeya[‖], Yasutomi Kamei[‡], and Yoshihiro Ogawa[‡§2]

From the [‡]Department of Molecular Medicine and Metabolism and the [§]Center of Excellence Program for Frontier Research on Molecular Destruction and Reconstitution of Tooth and Bone, Medical Research Institute, Tokyo Medical and Dental University, 2-3-10 Kanda-surugadai, Chiyoda-ku, Tokyo 101-0062, Japan, the [¶]Department of Medicine, Division of Atherosclerosis and Diabetes, National Cardiovascular Center Hospital, 5-7-1 Fujishirodai, Suita, Osaka 560-0005, Japan, and the [‖]Department of Cell Pathology, Graduate School of Medical Sciences, Kumamoto University, 1-1-1 Honjo, Kumamoto 860-8556, Japan

Monocyte chemoattractant protein-1 (MCP-1), an important chemokine whose expression is increased during the course of obesity, plays a role in macrophage infiltration into obese adipose tissue. This study was designed to elucidate the role of mitogen-activated protein kinase (MAPK) phosphatase-1 (MKP-1) in the induction of MCP-1 during the course of adipocyte hypertrophy. We examined the time course of MKP-1 and MCP-1 mRNA expression and extracellular signal-regulated kinase (ERK) phosphorylation in the adipose tissue from mice rendered mildly obese by a short term high fat diet. We also studied the role of MKP-1 in the induction of MCP-1 in 3T3-L1 adipocytes during the course of adipocyte hypertrophy. MCP-1 mRNA expression was increased, followed by ERK activation and down-regulation of MKP-1, an inducible dual specificity phosphatase to inactivate ERK, in the adipose tissue at the early stage of obesity induced by a short term high fat diet, when macrophages are not infiltrated. Down-regulation of MKP-1 preceded ERK activation and increased production of MCP-1 in 3T3-L1 adipocytes *in vitro* during the course of adipocyte hypertrophy. Adenovirus-mediated restoration of MKP-1 in hypertrophied 3T3-L1 adipocytes reduced the otherwise increased ERK phosphorylation, thereby leading to the significant reduction of MCP-1 mRNA expression. This study provides evidence that the down-regulation of MKP-1 is critical for increased production of MCP-1 during the course of adipocyte hypertrophy.

Evidence has accumulated suggesting that obesity is a state of chronic, low grade inflammation; it may represent a potential mechanism whereby obesity leads to the metabolic derangements (1–3). Previous studies demonstrated that the adipose tissue is markedly infiltrated by macrophages in several models of rodent obesities and human obese subjects (4, 5). Using an *in vitro* co-culture system composed of adipocytes and macrophages, we have provided evidence that a paracrine loop involving saturated free fatty acids (FFAs) and tumor necrosis factor-α (TNFα) derived from adipocytes and macrophages, respectively, establishes a vicious cycle that aggravates the inflammatory changes; *i.e.* marked up-regulation of pro-inflammatory cytokines such as monocyte chemoattractant protein-1 (MCP-1)[3] and TNFα and down-regulation of anti-inflammatory adiponectin (6, 7). These findings have led us to speculate that macrophages, when infiltrated, may participate in the inflammatory pathways that are activated in obese adipose tissue.

A previous study with bone marrow transplantation demonstrated that most macrophages in the adipose tissue are derived from the bone marrow (4). In this regard, adipose tissue expression of MCP-1, a major chemokine implicated in the control of monocyte recruitment to the site of inflammation, is increased during the progression of obesity (8, 9) and is roughly correlated with macrophage markers in the adipose tissue (5, 10). These findings suggest that increased production of MCP-1 may be an initial event at the early stage of obesity so as to accumulate macrophages in the adipose tissue. Recently, Kanda *et al.* and Kamei *et al.* (11, 12) have independently reported that MCP-1 plays a role in the recruitment of macrophages into obese adipose tissue. It is, therefore, important to know the molecular mechanism for increased production of MCP-1 at the early stage of obesity. Recent studies have demonstrated that multiple intracellular signaling pathways are activated in adipocytes during the

* This work was supported in part by a grant-in-aid for Scientific Research from the Ministry of Education, Culture, Sports, Science and Technology of Japan, and Ministry of Health, Labor, and Welfare of Japan, and research grants from the Astellas Foundation for Research on Metabolic Disorders, Astellas Foundation for Research on Medicinal Resources and The Ichiro Kanehara Foundation. The costs of publication of this article were defrayed in part by the payment of page charges. This article must therefore be hereby marked "*advertisement*" in accordance with 18 U.S.C. Section 1734 solely to indicate this fact.

[S] The on-line version of this article (available at http://www.jbc.org) contains supplemental Table S1 and Figs. S1–S5.

[1] Supported by the Tokyo Biochemical Research Foundation.

[2] To whom correspondence should be addressed: Dept. of Molecular Medicine and Metabolism, Medical Research Institute, Tokyo Medical and Dental University, 2-3-10 Kanda-surugadai, Chiyoda-ku, Tokyo 101-0062, Japan. Tel.: 81-3-5280-8108; Fax: 81-3-5280-8108; E-mail: ogawa.mmm@mri.tmd.ac.jp.

[3] The abbreviations used are: MCP-1, monocyte chemoattractant protein-1; MAPK, mitogen-activated protein kinase; MKP-1, mitogen-activated protein kinase phosphatase-1; ERK, extracellular signal-regulated kinase; JNK, c-Jun NH_2-terminal kinase; MEK, MAPK/ERK kinase; CAR, coxsackie-adenovirus receptor; WAT, white adipose tissue; GFP, green fluorescent protein; ER, endoplasmic reticulum; ROS, reactive oxygen species; SD, standard diet; HFD, high fat diet; IL, interleukin.

course of adipocyte hypertrophy *in vitro* and in obese adipose tissue *in vivo*. However, how the inflammatory pathways are activated in adipocytes at the early stage of obesity is still poorly understood.

Mitogen-activated protein kinases (MAPKs) including extracellular signal-regulated kinase (ERK), p38 MAPK, and c-Jun NH_2-terminal kinase (JNK) are activated in a variety of cellular processes (13). Once activated by the upstream kinases, *e.g.* MAPK/ERK kinase (MEK), MAPKs are rapidly inactivated by a family of protein phosphatases such as MAPK phosphatase-1 (MKP-1), an inducible dual specificity phosphatase (14, 15). Sakaue *et al.* showed previously that MKP-1 plays an essential role in 3T3-L1 adipocyte differentiation through ERK down-regulation (16). On the other hand, Bost *et al.* (17) reported that mice lacking ERK1 ($ERK1^{-/-}$ mice) are protected from high fat diet-induced obesity and insulin resistance. These findings, taken together, suggest that the MAPK pathways play an important role in the adipocyte proliferation and differentiation *in vitro* and *in vivo* (18).

Here we show that MCP-1 mRNA expression is increased, which is followed by ERK activation and MKP-1 down-regulation in the adipose tissue from mice rendered mildly obese by a short term high fat diet, when macrophages are not infiltrated. We also demonstrate that ERK activation through MKP-1 down-regulation is involved in increased production of MCP-1 in 3T3-L1 adipocytes during the course of adipocyte hypertrophy. This study provides evidence that MKP-1 down-regulation is critical for the inflammatory changes in hypertrophied adipocytes at the early stage of obesity, thereby suggesting that MKP-1 activation may offer a novel therapeutic strategy to treat or reduce the inflammatory changes in adipocytes during the progression of obesity.

EXPERIMENTAL PROCEDURES

Materials—Rabbit polyclonal antibodies against ERK, phospho-ERK, p38 MAPK, phospho-p38 MAPK, MEK1/2, phospho-MEK1/2, MEK inhibitors PD98059 and U0126, and a p38MAPK inhibitor SB203580 were purchased from Cell Signaling (Beverly, MA). Rabbit polyclonal antibodies against JNK, phospho-JNK, and MKP-1 and a mouse monoclonal antibody against Lamin A/C were purchased from Santa Cruz Biotechnology (Santa Cruz, CA). All other reagents were purchased from Sigma or Nacalai Tesque (Kyoto, Japan).

Animal Studies—Four-week-old male C57BL/6J mice were purchased from Charles River Laboratories Japan (Tokyo, Japan). The animals were housed in a temperature-, humidity-, and light- controlled room (12-h light and 12-h dark cycle) and allowed free access to water and chow. Five-week-old mice were fed either the standard chow (Oriental MF, 362 kcal/100 g, 5.4% energy as fat; Oriental Yeast, Tokyo, Japan) or high fat diet (D12492, 524 kcal/100 g, 60% energy as fat; Research Diets, New Brunswick, NJ) for 15 weeks. They were fasted for 1 h (12:00–13:00) and sacrificed to harvest the epididymal adipose tissue before (n = 10) and 2 weeks (n = 10), 4 weeks (n = 12), 6 weeks (n = 11), 8 weeks (n = 6), and 15 weeks (n = 4) after the experiments. All animal experiments were conducted according to the guidelines of Tokyo Medical and Dental University Committee on Animal Research (No. 0060026).

Histological Analysis—The epididymal WAT was fixed with neutral-buffered formalin and embedded in paraffin. Sections were stained with hematoxylin and eosin and studied under ×200 magnification to measure the adipocyte area using Win Roof software (Mitani Corporation, Tokyo, Japan) (19). Immunohistochemical study was carried out using 5-μm thick paraffin-embedded sections for macrophage marker F4/80 as previously described (20, 21).

Cell Culture—3T3-L1 preadipocytes (American Type Culture Collection, Manassas, VA) were maintained as described (6, 7). Differentiation of 3T3-L1 preadipocytes to adipocytes was described elsewhere (6, 7). Cells at day 8 and day 21 after the induction of differentiation were used as non-hypertrophied and hypertrophied adipocytes, respectively (6). Accumulation of triglyceride in adipocytes was detected by oil red O staining (19).

Measurement of Triglyceride Content—Triglyceride content in 3T3-L1 adipocytes was measured as previously reported (22). In brief, 3T3-L1 adipocytes in 35-mm dish were harvested, and cellular lipid was extracted by chloroform-methanol (2:1). After evaporation, precipitation was dissolved in isopropyl alcohol. Triglyceride content was measured using a colorimetric assay kit (triglyceride E-test Wako, Wako Pure Chemicals, Osaka, Japan) according to the manufacturer's instructions.

Quantitative Real-time PCR—Quantitative real-time PCR was performed with an ABI Prism 7000 Sequence Detection System using PCR Master Mix reagent kit (Applied Biosystems, Foster City, CA) as described (6, 19). Primers used were described in supplemental Table S1. Levels of mRNAs were normalized to those of housekeeping gene 36B4 mRNA.

ELISA—The MCP-1, IL-6, and adiponectin levels in culture supernatants were determined by the commercially available ELISA kits (MCP-1 and IL-6, R&D systems, Minneapolis, MN; adiponectin, Otsuka Pharmaceutical, Tokyo, Japan).

Immunoblot Assay—Nuclear and cytosolic extracts were prepared by using the Nuclear/Cytosol fractionation kit (BioVision, Mountain View, CA). Separation of nuclear and cytosolic proteins was confirmed by immunoblots with α-tubulin and lamin A/C antibodies, respectively. Whole cell lysates were prepared using buffer containing 50 mmol/liter HEPES (pH7.5), 150 mmol/liter NaCl, 100 mmol/liter sodium fluoride, 1 mmol/liter EGTA, 1 mmol/liter EDTA, 1% Triton X-100, 2 mmol/liter sodium vanadate, 2 mmol/liter phenylmethylsulfonyl fluoride, and protease inhibitor mixture (Sigma). Immunoblot assay was performed as described (6). Samples (10–20 μg protein/lane) were separated by 12.5% SDS-PAGE and electrophoretically transferred onto polyvinylidene difluoride filter membrane (PolyScreen; PerkinElmer, Wellesley, MA). After membranes were incubated with primary antibodies for 1 h at room temperature, immunoblots were developed with horseradish peroxidase-conjugated secondary antibodies (GE Healthcare Bio-Sciences, Piscataway, NJ) and a chemiluminescence kit (GE Healthcare Bio-Sciences). The signals were detected with LAS3000 (Fuji Photo Film, Tokyo, Japan).

Generation of 3T3-L1 Adipocytes Stably Expressing Coxsackie-Adenovirus Receptor (CAR)—A mouse CAR-expressing plasmid pcDNA3-CAR (23) was kindly provided by Dr. Hiroyuki Mizuguchi (National Institute of Biomedical Innovation, Osaka, Japan). The CAR retroviral expression vector (pMRX-CAR) was constructed by ligating the full-length CAR cDNA into the EcoR1 site of pMRX vector (24) and transfected into Plat-E packaging cells (25) using Lipofectamine2000 (Invitrogen) according to the manufacturer's instructions. Viral supernatants were harvested from 24 to 48 h after transfection and applied to 3T3-L1 adipocytes in Dulbecco's modified Eagle's medium containing 10% fetal bovine serum and 5 μg/ml of polybrene (Nacalai Tesque) in a final volume of 5 ml. The stable CAR-expressing 3T3-L1 adipocytes (CAR-3T3-L1 adipocytes) were obtained by 2 μg/ml of puromycin (Nacalai Tesque) selection.

Adenovirus-mediated Expression of MKP-1—The adenoviral vector expressing mouse MKP-1 (Ad-MKP-1) (26), kindly provided by Dr. Jeffery D. Molkentin (University of Cincinnati, Cincinnati, OH), was prepared using HEK293 cells and purified by VIRAPREP adenovirus purification kit (Virapur, LLC, San Diego, CA) as previously described (27). The GFP adenovirus (Ad-GFP; Clontech Laboratories, Palo Alto, CA) was used as a control. The CAR-3T3-L1 adipocytes at day 5 and day 18 after the induction of differentiation were transfected with Ad-MKP-1, incubated for 3 days, and harvested to be used for quantitative real-time PCR and immunoblot assay.

Statistical Analysis—Data are shown as means ± S.E. Statistical analysis was performed using the Student's *t* test and analysis of variance followed by Scheffe's test. $p < 0.05$ was considered statistically significant.

RESULTS

MCP-1 mRNA Expression in the Adipose Tissue from Mice with Diet-induced Obesity—Body weight was increased significantly in mice fed high fat diet for 2 weeks relative to those fed standard diet ($p < 0.01$) (Fig. 1*A*). The mice fed high fat diet weighed ~20% more than those fed standard diet for 15 weeks (29.7 ± 0.3 g *versus* 34.8 ± 1.9 g, $p < 0.05$). The weight of epididymal white adipose tissue (WAT) was significantly increased in mice fed high-fat diet for 2 weeks relative to those fed standard diet (0.26 ± 0.01 g *versus* 0.49 ± 0.04 g, $p < 0.01$). Histological examination revealed appreciable increase in adipocyte cell size in mice fed a high fat diet during the initial 2 weeks, which reached up to ~4-fold larger than that in mice fed standard diet after 15 weeks (Fig. 1*B*). There were no appreciable infiltration of macrophages in the adipose tissue up to 8 weeks after the experiment, after which interstitial cells stained with F4/80, a marker of activated macrophages, appeared in mice fed high fat diet (Fig. 1*C*). Correspondingly, F4/80 mRNA expression was also increased in the epididymal WAT in mice fed high fat diet for 15 weeks relative to those fed standard diet (Fig. 1*D*, *left*). In mice fed high fat diet, MCP-1 mRNA expression was increased as early as 4 weeks and gradually increased up to 15 weeks after the experiment (Fig. 1*D*, *right*). These observations indicate that MCP-1 mRNA expression is increased prior to macrophage infiltration at the early stage of obesity.

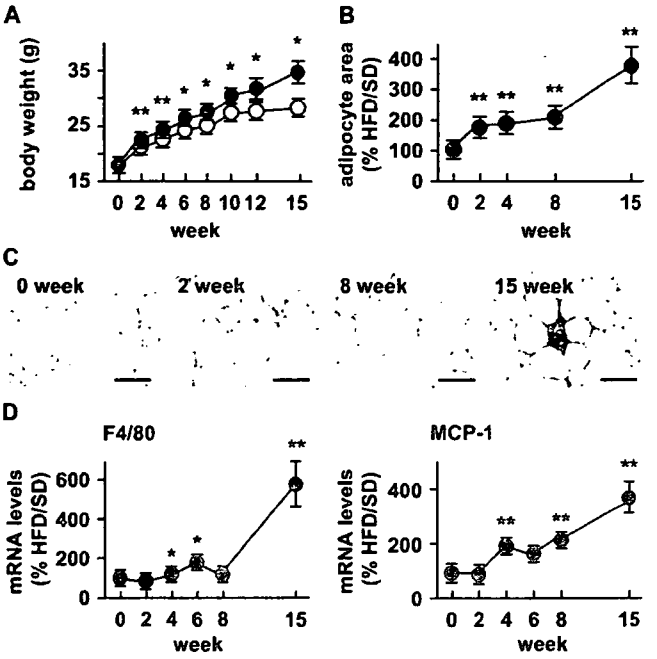

FIGURE 1. **Time course of adipocyte hypertrophy and macrophage infiltration in mice with diet-induced obesity.** Five-week-old male C57BL/6J mice were fed either SD or HFD for 15 weeks. *A*, time course of body weight. *Open circle*, SD; *closed circle*, HFD. *B*, time course of adipocyte area. *C*, macrophage marker F4/80 immunostaining of the epididymal WAT in diet-induced obese mice. Original magnification, ×200. *Scale bars*, 100 μm. *D*, time courses of F4/80 and MCP-1 mRNA expression. Data in *B* and *D* are expressed as the ratio of changes in mice fed HFD to those in mice fed SD. *, $p < 0.05$; **, $p < 0.01$ *versus* SD, $n = 4$–12 at each time point.

Dysregulation of Adipocytokine Production during the Course of Adipocyte Hypertrophy—To explore the molecular mechanisms underlying adipocyte hypertrophy, we cultured 3T3-L1 adipocytes up to 21 days after the induction of differentiation; they exhibited a gradual increase in lipid accumulation from day 8 to day 21 during the course of adipocyte hypertrophy as revealed by oil-red O staining (Fig. 2*A*) and triglyceride content (Fig. 2*B*). In this study, insulin-induced glucose uptake was preserved up to day 21 (supplemental Fig. S1).

Quantitative real-time PCR analysis revealed that MCP-1 mRNA expression was significantly increased up to day 21, ~6-fold higher than that in 3T3-L1 adipocytes (day 8) ($p < 0.01$), in parallel with increased cell size and lipid accumulation (Fig. 2*C*). Expression of IL-6 mRNA was also increased during the course of adipocyte hypertrophy. The IL-6 mRNA levels in 3T3-L1 adipocytes (day 21) were ~5-fold higher than those in 3T3-L1 adipocytes (day 8) ($p < 0.01$). By contrast, adiponectin mRNA expression showed significant reduction (up to 30%) during the course of adipocyte hypertrophy ($p < 0.01$). The MCP-1, IL-6, and adiponectin concentrations in the culture media were roughly parallel to their respective mRNA levels (Fig. 2*D*). The expression patterns of adipocytokines in hypertrophied 3T3-L1 adipocytes (day 21) were similar to those found in obese adipose tissue. We also confirmed that mRNA expression patterns of adipogenesis-related markers such as peroxisome proliferator-activated receptor γ2 (PPARγ2), adipocyte fatty acid-binding protein (aP2), fatty-acid transport protein 1 (FATP1), and CCAAT/enhancer-binding protein α

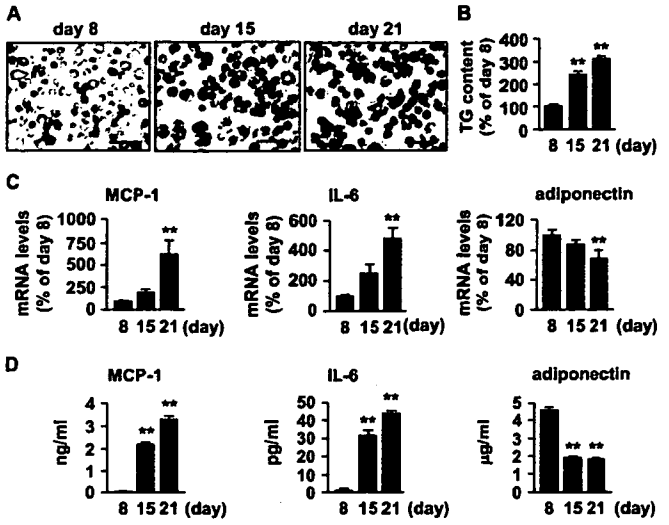

FIGURE 2. **Changes in adipocytokine expression during the course of adipocyte hypertrophy *in vitro*.** *A*, morphological changes of 3T3-L1 adipocytes during the course of adipocyte hypertrophy (day 8-day 21) as revealed by oil-red O staining. Original magnification, ×200. *Scale bars*, 100 μm. *B*, triglyceride accumulation in 3T3-L1 adipocytes during the course of adipocyte hypertrophy. *C* and *D*, changes in adipocytokine mRNA expression (*C*) and secretion (*D*) in 3T3-L1 adipocytes during the course of adipocyte hypertrophy. **, $p < 0.01$ *versus* day 8. $n = 4$.

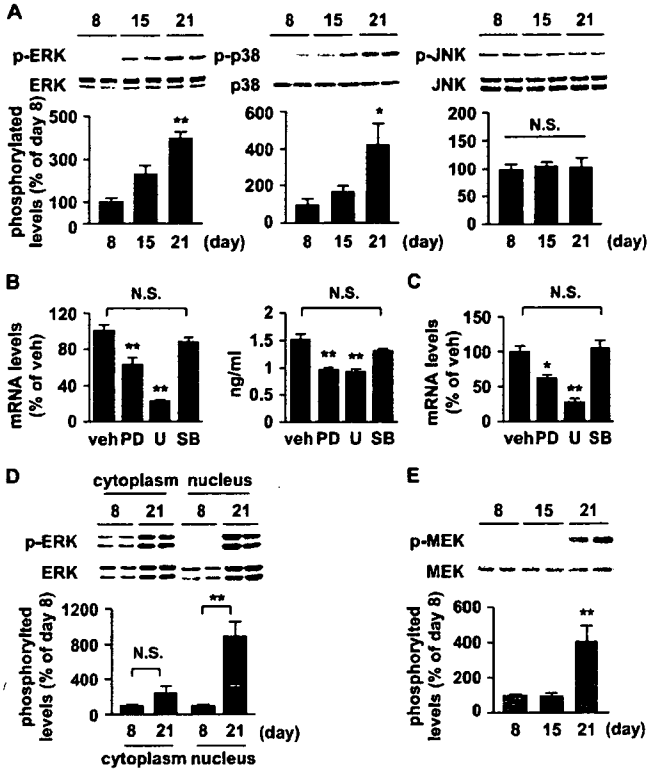

FIGURE 3. **Role of MAP kinases in MCP-1 mRNA expression in hypertrophied adipocytes.** *A*, phosphorylation of MAP kinases during the course of adipocyte hypertrophy. Representative immunoblots of ERK, p38 MAPK and JNK quantification of phosphorylation levels. *, $p < 0.05$; **, $p < 0.01$ *versus* day 8. $n = 4$. *B*, effect of 24-h-treatment with MAP kinase inhibitors on MCP-1 mRNA expression (*left*) and secretion (*right*) in hypertrophied 3T3-L1 adipocytes (day 21). *PD*, PD98059, 20 μmol/liter; *U*, U0126, 10 μmol/liter; *SB*, SB203580, 10 μmol/liter. **, $p < 0.01$ *versus* vehicle treated day 21. $n = 6$. *N.S.*, not significant. *C*, effect of 6-h-treatment with MAPK inhibitors on MCP-1 mRNA expression in hypertrophied 3T3-L1 adipocytes (day 21). *D*, phosphorylation of ERK in the cytosolic and nuclear fractions from non-hypertrophied (day 8) and hypertrophied (day 21) 3T3-L1 adipocytes. Representative immunoblots of ERK and quantification of phosphorylation levels. *E*, phosphorylation of MEK during the course of adipocyte hypertrophy. Representative immunoblots of MEK and quantification of phosphorylation levels. **, $p < 0.01$ *versus* day 8. $n = 4-6$.

(C/EBPα) in hypertrophied 3T3-L1 adipocytes were consistent with those in obese adipose tissue (supplemental Fig. S2). In this study, we used 3T3-L1 adipocytes cultured for 8 and 21 days after differentiation as non-hypertrophied (day 8) and hypertrophied (day 21) adipocytes, respectively.

Activation of MAPK Pathways during the Course of Adipocyte Hypertrophy—To explore the role of MAPK activation in the dysregulation of MCP-1 production during the course of adipocyte hypertrophy, we examined phosphorylation of ERK, p38 MAPK, and JNK in 3T3-L1 adipocytes during the course of adipocyte hypertrophy. Immunoblot analysis revealed that phosphorylation of ERK and p38 MAPK is increased in hypertrophied adipocytes relative to non-hypertrophied adipocytes (Fig. 3*A*). In this study, there was no significant induction of phosphorylation of JNK during the course of adipocyte hypertrophy (Fig. 3*A*). Treatment of hypertrophied adipocytes with MEK inhibitors, PD98059 and U0126, for 24 h significantly reduced MCP-1 mRNA levels (Fig. 3*B* left, $p < 0.01$) and secretion in the culture media (Fig. 3*B* right, $p < 0.01$). Moreover, the effect of the MEK inhibitors on MCP-1 mRNA expression was observed as early as 6 h after the treatment (Fig. 3*C*). Furthermore, phosphorylation of ERK was increased in the nuclear fraction rather than in the cytosolic fraction from hypertrophied adipocytes (Fig. 3*D*, $p < 0.01$). We also confirmed that phosphorylation of MEK is increased in hypertrophied adipocytes (Fig. 3*E*, $p < 0.01$). On the other hand, no such inhibitory effect was observed when treated with a p38 MAPK inhibitor, SB203580 (Fig. 3, *B* and *C*). These observations suggest that increased mRNA expression and secretion of MCP-1 in hypertrophied adipocytes are due at least in part to MEK-ERK activation.

MKP-1 Down-regulation during the Course of Adipocyte Hypertrophy—We next examined expression of members of the MKP family during the course of adipocyte hypertrophy. Interestingly, we detected substantial amounts of MKP-1 mRNA and protein in non-hypertrophied adipocytes, which are markedly down-regulated in hypertrophied adipocytes (Fig. 4, *A* and *B*, $p < 0.05$). There were no obvious changes in MKP-2 and MKP-3 mRNA levels during the course of adipocyte hypertrophy (Fig. 4*A*). We also observed that MKP-1 mRNA expression is significantly down-regulated in the adipose tissue from mice fed high fat diet for 2- and 4-weeks relative to those fed standard diet (Fig. 4*C*, $p < 0.05$). In addition, phosphorylation of ERK was significantly increased in the adipose tissue from mice that received 4-, 6-, 8-, and 15-week high fat diet relative to those fed standard diet (Fig. 4*D*, $p < 0.05$). These observations, taken together, suggest that MKP-1 is down-regulated in hypertrophied adipocytes, which is accompanied by ERK activation *in vivo*.

Generation of CAR-3T3-L1 Adipocytes—Because MKP-1 down-regulation may be responsible for the induction of MCP-1 during the course of adipocyte hypertrophy, we next examined the effect of MKP-1 restoration on ERK activity and

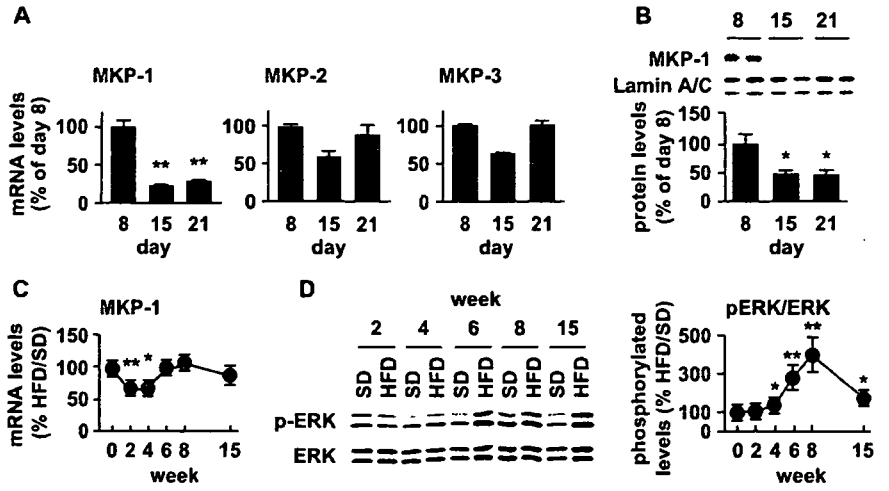

FIGURE 4. **Changes in MKP-1 expression during the course of adipocyte hypertrophy *in vitro* and *in vivo*.** *A*, changes in mRNA expression of MKP family during the course of adipocyte hypertrophy. $n = 6$. *B*, changes in MKP-1 protein levels in 3T3-L1 adipocytes during the course of adipocyte hypertrophy. Representative immunoblots of MKP-1 and quantification of protein levels. $n = 4$. *, $p < 0.05$; **, $p < 0.01$ *versus* day 8. *C* and *D*, time course of MKP-1 mRNA expression (*C*) and ERK phosphorylation (*D*) levels in mice with diet-induced obesity. Representative immunoblots of ERK and quantification of phosphorylation levels. Data in *C* and *D* are expressed as the ratio of changes in mice fed HFD to those in mice fed SD. *, $p < 0.05$; **, $p < 0.01$ *versus* SD. $n = 4-12$ at each time point.

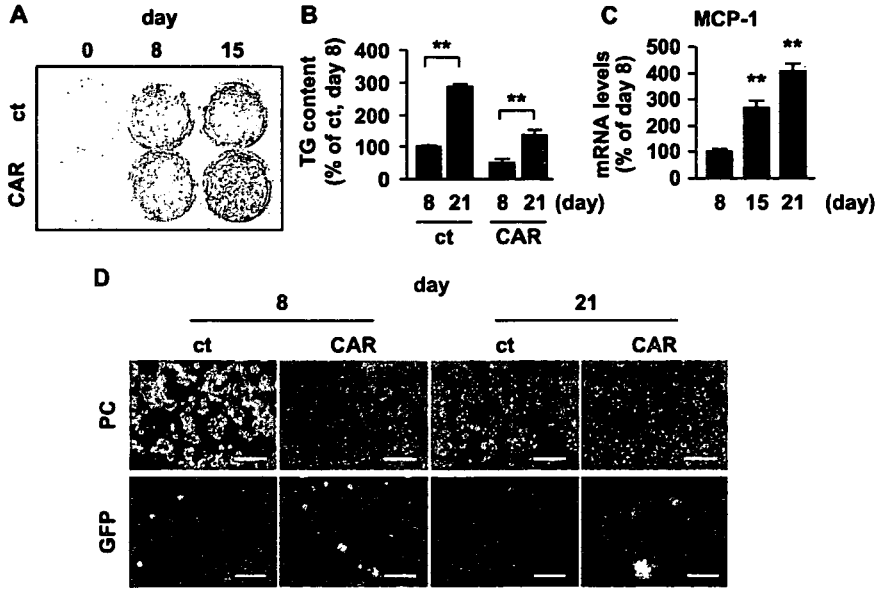

FIGURE 5. **Generation of 3T3-L1 adipocytes stably expressing CAR (CAR-3T3-L1 adipocytes).** *A* and *B*, lipid accumulation of CAR-3T3-L1 adipocytes and control 3T3-L1 adipocytes (*ct*) during the course of adipocyte differentiation and hypertrophy as revealed by oil-red O staining (*A*) and triglyceride content (*B*). *C*, changes in MCP-1 mRNA expression in CAR-3T3-L1 adipocytes. *D*, efficiency of adenovirus-mediated gene transfer in CAR-3T3-L1 adipocytes using Ad-GFP. *PC*, phase contrast view; *GFP*, GFP fluorescence view. Original magnification, ×200. *Scale bars*, 100 μm. **, $p < 0.01$ *versus* day 8. $n = 4$.

MCP-1 mRNA expression in hypertrophied adipocytes. Because hypertrophied 3T3-L1 adipocytes are difficult to transfect with plasmid- or even virally encoded genes, we generated CAR-3T3-L1 adipocytes as described under "Experimental Procedures." There was no obvious difference in lipid accumulation between CAR-3T3-L1 and 3T3-L1 adipocytes without retroviral infection (control 3T3-L1 adipocytes) (Fig. 5, *A* and *B*) during the course of adipocyte differentiation and hypertrophy. We also confirmed no appreciable difference in mRNA expression of adipogenesis-related markers and adipocytokines between the cells (supplemental Fig. S3). Similar to control 3T3-L1 adipocytes, CAR-3T3-L1 adipocytes exhibited the up-regulation of MCP-1 during the course of adipocyte hypertrophy (Fig. 5*C*). The transfection efficiency was markedly increased in CAR-3T3-L1 adipocytes relative to control 3T3-L1 adipocytes as judged by Ad-GFP infection (Fig. 5*D*).

Effect of MKP-1 Restoration in Hypertrophied Adipocytes—Infection with Ad-MKP-1 significantly increased MKP-1 mRNA expression in hypertrophied CAR-3T3-L1 adipocytes (Fig. 6*A*, *left*). We confirmed that MKP-1 protein levels in hypertrophied CAR-3T3-L1 adipocytes infected with Ad-MKP-1 are roughly comparable to those found in non-hypertrophied CAR-3T3-L1 adipocytes (Fig. 6*A*, *right*). In this setting, MKP-1 restoration in hypertrophied CAR-3T3-L1 adipocytes resulted in a marked reduction of ERK phosphorylation (Fig. 6*B*, $p < 0.05$) and MCP-1 mRNA expression (Fig. 6*C*, $p < 0.01$), which is roughly comparable to those found in non-hypertrophied CAR-3T3-L1 adipocytes. Interestingly, adiponectin mRNA expression was significantly increased and IL-6 mRNA expression tended to be reduced in hypertrophied CAR-3T3-L1 adipocytes with Ad-MKP-1 infection (supplemental Fig. S4), suggesting the anti-inflammatory effect of MKP-1 in hypertrophied adipocytes. Of note, there was no obvious difference in mRNA expression of adipogenesis-related markers by Ad-MKP-1 infection (supplemental Fig. S4). We also confirmed that Ad-MKP-1 infection does not affect lipid accumulation and insulin-induced glucose uptake in hypertrophied CAR-3T3-L1 (supplemental Fig. S5). These observations, taken together, indicate that restoration of MKP-1 does not affect adipocyte differentiation and hypertrophy but improves the overall inflammatory changes in hypertrophied adipocytes.

DISCUSSION

Recent studies showed that obese adipose tissue is characterized by increased infiltration of macrophages, suggesting that

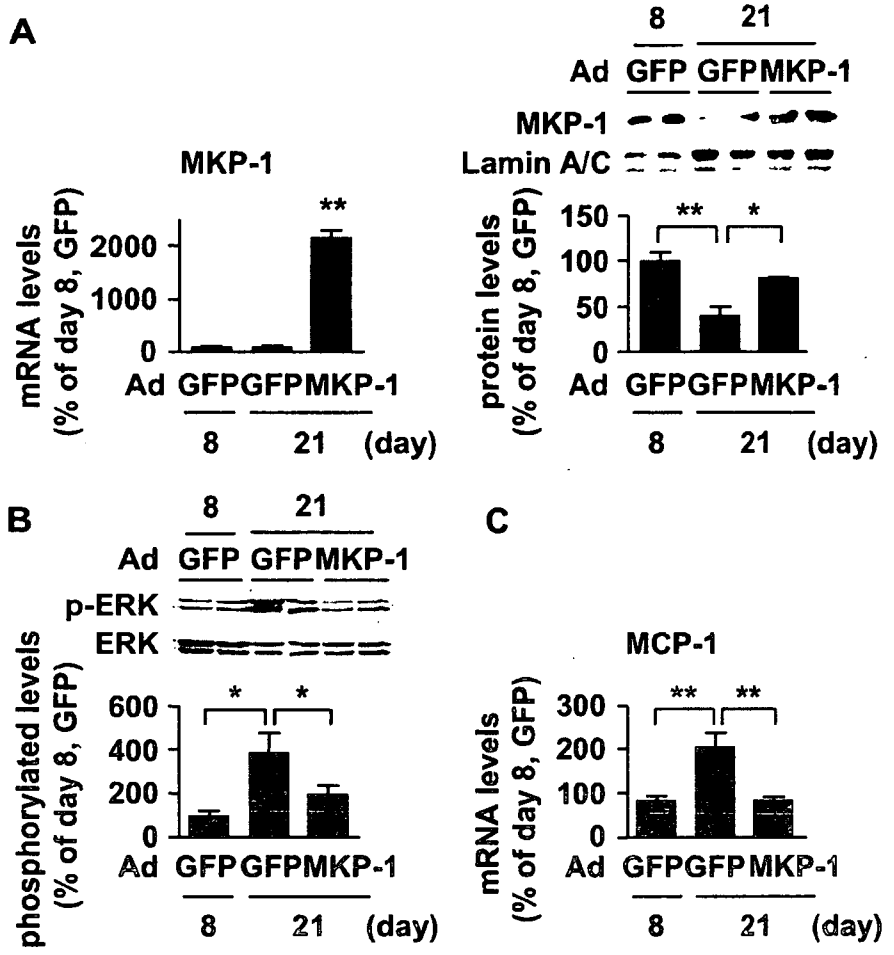

FIGURE 6. **Effect of MKP-1 restoration on ERK phosphorylation and MCP-1 mRNA expression in hypertrophied adipocytes.** *A*, adenovirus-mediated restoration of MKP-1 in hypertrophied CAR-3T3-L1 adipocytes (day 21). Changes in MKP-1 mRNA (*left*) and protein (*right*) expression. Representative immunoblots of MKP-1 and quantification of protein levels. *B* and *C*, effect of MKP-1 restoration on ERK phosphorylation (*B*) and MCP-1 mRNA expression (*C*). *, $p < 0.05$; **, $p < 0.01$ *versus* Ad-GFP, (day 21). $n = 6$.

the inflammatory changes induced by the cross-talk between adipocytes and macrophages are critical for the pathophysiology of obesity and thus the metabolic syndrome (4, 5). The molecular mechanisms underlying the recruitment of macrophages into obese adipose tissue have not fully been elucidated, but there is considerable evidence suggesting the involvement of MCP-1, which is increased during the course of obesity (8, 9). It is, therefore, important to know how MCP-1 is increased in hypertrophied adipocytes at the early stage of obesity, when macrophages are not infiltrated. This study was designed to elucidate the signaling pathway that mediates increased production of MCP-1 at the early stage of obesity.

In this study, we found that expression of MCP-1 mRNA is increased in the adipose tissue from mice rendered mildly obese by a short term high fat diet. Histologically, there is marked increase in adipocyte cell size with no obvious macrophage infiltration, suggesting that MCP-1 mRNA expression is increased in the adipose tissue prior to macrophage accumulation *in vivo*. Two recent studies with transgenic mice overexpressing MCP-1 in the adipose tissue and/or MCP-1-deficient mice showed that MCP-1 plays a role in the recruitment of macrophages into obese adipose tissue (11, 12). Furthermore, Weisberg *et al.* (28) reported the attenuation of macrophage content and inflammatory changes in the adipose tissue from mice lacking C-C motif chemokine receptor-2, a major receptor for MCP-1, during a long term high fat diet. Together with recent evidence that MCP-1 mRNA expression and secretion in primary cultured adipocytes from obese subjects are positively correlated with their cell size (29), our data herein support the concept that increased production of MCP-1 in hypertrophied adipocytes at the early stage of obesity contributes to increased infiltration of macrophages into the adipose tissue at the late stage of obesity.

There are multiple intracellular signaling pathways activated in adipocytes during the course of adipocyte hypertrophy. The data of this study demonstrate that 3T3-L1 adipocytes, when cultured alone up to 21 days after differentiation, is capable of up-regulating MCP-1 and IL-6 and down-regulating adiponectin in parallel with increased cell size and lipid accumulation, which are comparable to those in obese adipose tissue. Moreover, mRNA expression patterns of some adipogenesis-related markers are also roughly parallel to those in obese adipose tissue, suggesting that 3T3-L1 adipocytes cultured from day 8 to day 21 serve as the useful *in vitro* experimental model system to investigate the molecular mechanism for the dysregulation of adipocytokine production during the course of adipocyte hypertrophy.

In this study, we observed that ERK and p38 MAPK are activated in hypertrophied 3T3-L1 adipocytes. Moreover, increased production of MCP-1 is significantly suppressed by MEK inhibitors as early as 6 h after the treatment, but not by a p38 MAPK inhibitor. We also demonstrated that ERK phosphorylation is significantly increased in the nuclear fraction but not in cytosolic fraction obtained from non-hypertrophied (day 8) and hypertrophied (day 21) 3T3-L1 adipocytes, suggesting that ERK activation occurs mostly in the nucleus rather than in the cytoplasm of adipocytes during the course of adipocyte hypertrophy. These observations are consistent with the concept that MKP-1 acts as a negative regulator of MAPKs within the nucleus (30). Furthermore, we observed that phosphorylation of MEK is increased in hypertrophied adipocytes. Together with a recent report that MAPKs are involved in the regulation of MCP-1 in human adipose tissue (31), these observations suggest that increased production of MCP-1 in hypertrophied adipocytes is mediated at least in part thorough MEK-ERK activa-

tion. In this regard, using the TRANSFAC (6.0) data base, we also searched for transcriptional factor binding sites in the mouse, rat, and human MCP-1 promoter and found a consensus AP-1 binding site 3–4-kb upstream of the transcriptional start site. Moreover, there are previous reports showing that cytokine-induced MCP-1 is mediated at least in part through the activation of ERK and AP-1 (32, 33). It is, therefore, conceivable that decrease in MKP-1 leads to the activation of ERK and AP-1 transcriptional activity within the nucleus, thereby increasing MCP-1 production during the course of adipocyte hypertrophy.

In this study, we demonstrate for the first time that both MKP-1 mRNA and protein levels are significantly down-regulated during the course of adipocyte hypertrophy *in vitro*. Moreover, restoration of MKP-1 in hypertrophied adipocytes reduces the otherwise increased ERK phosphorylation and thus MCP-1 mRNA expression. These observations, taken together, suggest that ERK activation through MKP-1 down-regulation is involved in increased production of MCP-1 in 3T3-L1 adipocytes during the course of adipocyte hypertrophy. The above discussion is consistent with the *in vivo* observation that ERK is activated, which is followed by MKP-1 down-regulation in the adipose tissue at the early stage of obesity, when there is no appreciable macrophage infiltration. Thus, reduced MKP-1 expression may be one of the early events during the progression of obesity *in vivo*, thereby leading to increased production of MCP-1 through the activation of ERK. In this regard, constitutive activation of ERK as a result of low induction of MKP-1 confers stronger resistance of immortalized cells than that of normal human fibroblasts to a cancer therapy called photodynamic therapy (34, 35). It is also noteworthy that MKP-1 expression is down-regulated in human ovarian cancer cell lines, where its forced re-expression reduces their malignant potential, suggesting the role of MKP-1 in the progression of human ovarian cancer (36). Thus, imbalance between MKP-1 and MEK activities as a result of MKP-1 down-regulation may cause ERK activation, thereby leading to increased production of MCP-1 in hypertrophied adipocytes.

It is also important to know the upstream signaling pathways responsible for MKP-1 down-regulation during the course of adipocyte hypertrophy. Recent studies have suggested the involvement of multiple intracellular signaling pathways in the inflammatory changes in adipocytes *in vitro* and in obese adipose tissue *in vivo*. For instance, Özcan *et al.* (37) reported that obesity is associated with the induction of ER stress predominantly in the adipose tissue and liver and demonstrated that ER stress is a central feature of obesity-related insulin resistance and type 2 diabetes. On the other hand, Furukawa *et al.* showed that ROS production is increased in parallel with lipid accumulation in 3T3-L1 adipocytes and that oxidative stress induces the dysregulation of adipocytokine production (38). It is, therefore, interesting to investigate the relationship among ER stress induction, ROS production, and MKP-1 activation during the course of adipocyte hypertrophy and/or at the early stage of obesity. Lin *et al.* (39, 40) demonstrated previously that MKP-1 degradation via the ubiquitin-proteasome pathway is stimulated by ERK, thereby leading to the sustained activation of ERK. Whether MKP-1 is thus down-regulated in hypertrophied adipocytes or not must await further investigations.

During the course of this study, Wu *et al.* (41) have reported that mice deficient in MKP-1 (MKP-1$^{-/-}$ mice) exhibit enhanced MAPK activity in the adipose tissue, reduced adipocyte cell size relative to wild-type littermates, and resistance to diet-induced obesity as a result of increased lipid metabolism in the liver and oxygen consumption in the skeletal muscle. Using mice with congenital deficiency of MKP-1, however, the authors did not address the role of MKP-1 in adipocytes during the course of adipocyte hypertrophy or at the early stage of obesity. In this regard, Bost *et al.* (17) reported that ERK1$^{-/-}$ mice have decreased adiposity and fewer adipocytes than wild-type littermates, and are resistant to high fat diet-induced obesity and insulin resistance. In this study, we demonstrated that ERK activation through the down-regulation of MKP-1 plays a role in increased production of MCP-1 in hypertrophied adipocytes during the course of obesity. It is, therefore, tempting to speculate that ERK activation through the down-regulation of MKP-1 plays an important role in the regulation of adipocyte differentiation, adiposity, and high fat diet-induced obesity *in vivo*. In this study, we also found that restoration of MKP-1 improves the dysregulation of adipocytokine production in hypertrophied adipocytes, which may improve obesity-related insulin resistance via adipocytokine mechanism *in vivo*. The pathophysiologic role of MKP-1 down-regulation in hypertrophied adipocytes at the early stage of obesity *in vivo* must await further investigation.

To obtain hypertrophied 3T3-L1 adipocytes whose MKP-1 levels are restored to those of non-hypertrophied 3T3-L1, we tried to produce 3T3-L1 adipocytes stably expressing MKP-1 using the retrovirus vector and observed that they are unable to differentiate into lipid-laden mature adipocytes.[4] This is consistent with the concept that ERK should be on and off properly during adipogenesis *in vitro* (16, 42). Although the adenoviral vector has been widely used for the introduction of exogenous genes in non-proliferating cells, 3T3-L1 adipocytes, particularly when hypertrophied, are transfected with less efficiency because of the scarcity of CAR (43–45). In this study, we generated 3T3-L1 adipocytes stably expressing CAR (or CAR-3T3-L1 adipocytes), which is infected with the adenoviral expression vector with ease, even after being hypertrophied. Importantly, there are no appreciable differences in adipogenesis, lipid accumulation, and adipocytokine expression during the course of adipocyte differentiation and hypertrophy between CAR-3T3-L1 adipocytes and control 3T3-L1 adipocytes. This study has verified the usefulness of CAR-3T3-L1 adipocytes as the unique experimental tool to investigate the molecular basis for adipocyte differentiation and hypertrophy.

In conclusion, this study represents the first demonstration that ERK activation through MKP-1 down-regulation is involved in increased production of MCP-1 in adipocytes at the early stage of obesity. The data of this study suggest that MKP-1 activation may offer a novel therapeutic strategy to reduce the otherwise increased production of MCP-1 in hypertrophied

[4] A. Ito, T. Suganami, and Y. Ogawa, unpublished data.

adipocytes at the early stage of obesity and thus macrophage infiltration into the adipose tissue at the late stage of obesity.

Acknowledgments—We thank Dr. Hiroshi Nishina for critical reading of the manuscript. We thank Dr. Toshio Kitamura for Plat-E, Dr. Hiroyuki Mizuguchi for pcDNA3-CAR, Dr. Shoji Yamaoka for pMRX, and Dr. Jeffery D. Molkentin for MKP-1 adenoviral expression vector. We are also grateful to the members of the Ogawa laboratory for discussions.

REFERENCES

1. Dandona, P., Aljada, A., and Bandyopadhyay, A. (2004) *Trends Immunol.* **25,** 4–7
2. Wellen, K. E., and Hotamisligil, G. S. (2005) *J. Clin. Investig.* **115,** 1111–1119
3. Berg, A. H., and Scherer, P. E. (2005) *Circ. Res.* **96,** 939–949
4. Weisberg, S. P., McCann, D., Desai, M., Rosenbaum, M., Leibel, R. L., and Ferrante, A. W., Jr. (2003) *J. Clin. Investig.* **112,** 1796–1808
5. Xu, H., Barnes, G. T., Yang, Q., Tan, G., Yang, D., Chou, C. J., Sole, J., Nichols, A., Ross, J. S., Tartaglia, L. A., and Chen, H. (2003) *J. Clin. Investig.* **112,** 1821–1830
6. Suganami, T., Nishida, J., and Ogawa, Y. (2005) *Arterioscler. Thromb. Vasc. Biol.* **25,** 2062–2068
7. Suganami, T., Tanimoto-Koyama, K., Nishida, J., Itoh, M., Yuan, X., Mizuarai, S., Kotani, H., Yamaoka, S., Miyake, K., Aoe, S., Kamei, Y., and Ogawa, Y. (2007) *Arterioscler. Thromb. Vasc. Biol.* **27,** 84–91
8. Chen, A., Mumick, S., Zhang, C., Lamb, J., Dai, H., Weingarth, D., Mudgett, J., Chen, H., MacNeil, D. J., Reitman, M. L., and Qian, S. (2005) *Obes. Res.* **13,** 1311–1320
9. Takahashi, K., Mizuarai, S., Araki, H., Mashiko, S., Ishihara, A., Kanatani, A., Itadani, H., and Kotani, H. (2003) *J. Biol. Chem.* **278,** 46654–46660
10. Cancello, R., Henegar, C., Viguerie, N., Taleb, S., Poitou, C., Rouault, C., Coupaye, M., Pelloux, V., Hugol, D., Bouillot, J. L., Bouloumie, A., Barbatelli, G., Cinti, S., Svensson, P. A., Barsh, G. S., Zucker, J. D., Basdevant, A., Langin, D., and Clement, K. (2005) *Diabetes* **54,** 2277–2286
11. Kamei, N., Tobe, K., Suzuki, R., Ohsugi, M., Watanabe, T., Kubota, N., Ohtsuka-Kowatari, N., Kumagai, K., Sakamoto, K., Kobayashi, M., Yamauchi, T., Ueki, K., Oishi, Y., Nishimura, S., Manabe, I., Hashimoto, H., Ohnishi, Y., Ogata, H., Tokuyama, K., Tsunoda, M., Ide, T., Murakami, K., Nagai, R., and Kadowaki, T. (2006) *J. Biol. Chem.* **281,** 26602–26614
12. Kanda, H., Tateya, S., Tamori, Y., Kotani, K., Hiasa, K., Kitazawa, R., Kitazawa, S., Miyachi, H., Maeda, S., Egashira, K., and Kasuga, M. (2006) *J. Clin. Investig.* **116,** 1494–1505
13. Johnson, G. L., and Lapadat, R. (2002) *Science* **298,** 1911–1912
14. Farooq, A., and Zhou, M. M. (2004) *Cell. Signal.* **16,** 769–779
15. Keyse, S. M. (2000) *Curr. Opin. Cell Biol.* **12,** 186–192
16. Sakaue, H., Ogawa, W., Nakamura, T., Mori, T., Nakamura, K., and Kasuga, M. (2004) *J. Biol. Chem.* **279,** 39951–39957
17. Bost, F., Aouadi, M., Caron, L., Even, P., Belmonte, N., Prot, M., Dani, C., Hofman, P., Pages, G., Pouyssegur, J., Le Marchand-Brustel, Y., and Binetruy, B. (2005) *Diabetes* **54,** 402–411
18. Rosen, E. D., and MacDougald, O. A. (2006) *Nat. Rev. Mol. Cell Biol.* **7,** 885–896
19. Kouyama, R., Suganami, T., Nishida, J., Tanaka, M., Toyoda, T., Kiso, M., Chiwata, T., Miyamoto, Y., Yoshimasa, Y., Fukamizu, A., Horiuchi, M., Hirata, Y., and Ogawa, Y. (2005) *Endocrinology* **146,** 3481–3489
20. Suganami, T., Mieda, T., Itoh, M., Shimoda, Y., Kamei, Y., and Ogawa, Y. (2007) *Biochem. Biophys. Res. Commun.* **354,** 45–49
21. Jinnouchi, K., Terasaki, Y., Fujiyama, S., Tomita, K., Kuziel, W. A., Maeda, N., Takahashi, K., and Takeya, M. (2003) *J. Pathol.* **200,** 406–416
22. Kamon, J., Naitoh, T., Kitahara, M., and Tsuruzoe, N. (2001) *Cell. Signal* **13,** 105–109
23. Hosono, T., Mizuguchi, H., Katayama, K., Koizumi, N., Kawabata, K., Yamaguchi, T., Nakagawa, S., Watanabe, Y., Mayumi, T., and Hayakawa, T. (2005) *Gene (Amst.)* **348,** 157–165
24. Saitoh, T., Nakayama, M., Nakano, H., Yagita, H., Yamamoto, N., and Yamaoka, S. (2003) *J. Biol. Chem.* **278,** 36005–36012
25. Morita, S., Kojima, T., and Kitamura, T. (2000) *Gene Ther.* **7,** 1063–1066
26. Bueno, O. F., De Windt, L. J., Lim, H. W., Tymitz, K. M., Witt, S. A., Kimball, T. R., and Molkentin, J. D. (2001) *Circ. Res.* **88,** 88–96
27. Suganami, E., Takagi, H., Ohashi, H., Suzuma, K., Suzuma, I., Oh, H., Watanabe, D., Ojima, T., Suganami, T., Fujio, Y., Nakao, K., Ogawa, Y., and Yoshimura, N. (2004) *Diabetes* **53,** 2443–2448
28. Weisberg, S. P., Hunter, D., Huber, R., Lemieux, J., Slaymaker, S., Vaddi, K., Charo, I., Leibel, R. L., and Ferrante, A. W., Jr. (2006) *J. Clin. Investig.* **116,** 115–124
29. Skurk, T., Alberti-Huber, C., Herder, C., and Hauner, H. (2006) *J. Clin. Endocrinol. Metab.* **92,** 1023–1033
30. Camps, M., Nichols, A., and Arkinstall, S. (2000) *FASEB J.* **14,** 6–16
31. Fain, J. N., and Madan, A. K. (2005) *Int. J. Obes. (Lond.)* **29,** 1299–1307
32. Marumo, T., Schini-Kerth, V. B., and Busse, R. (1999) *Diabetes* **48,** 1131–1137
33. Yoshimura, H., Nakahama, K., Safronova, O., Tanaka, N., Muneta, T., and Morita, I. (2006) *Inflamm. Res.* **55,** 543–549
34. Barry, O. P., Mullan, B., Sheehan, D., Kazanietz, M. G., Shanahan, F., Collins, J. K., and O'Sullivan, G. C. (2001) *J. Biol. Chem.* **276,** 15537–15546
35. Tong, Z., Singh, G., and Rainbow, A. J. (2002) *Cancer Res.* **62,** 5528–5535
36. Manzano, R. G., Montuenga, L. M., Dayton, M., Dent, P., Kinoshita, I., Vicent, S., Gardner, G. J., Nguyen, P., Choi, Y. H., Trepel, J., Auersperg, N., and Birrer, M. J. (2002) *Oncogene* **21,** 4435–4447
37. Özcan, U., Cao, Q., Yilmaz, E., Lee, A. H., Iwakoshi, N. N., Ozdelen, E., Tuncman, G., Gorgun, C., Glimcher, L. H., and Hotamisligil, G. S. (2004) *Science* **306,** 457–461
38. Furukawa, S., Fujita, T., Shimabukuro, M., Iwaki, M., Yamada, Y., Nakajima, Y., Nakayama, O., Makishima, M., Matsuda, M., and Shimomura, I. (2004) *J. Clin. Investig.* **114,** 1752–1761
39. Lin, Y. W., Chuang, S. M., and Yang, J. L. (2003) *J. Biol. Chem.* **278,** 21534–21541
40. Lin, Y. W., and Yang, J. L. (2006) *J. Biol. Chem.* **281,** 915–926
41. Wu, J. J., Roth, R. J., Anderson, E. J., Hong, E. G., Lee, M. K., Choi, C. S., Neufer, P. D., Shulman, G. I., Kim, J. K., and Bennett, A. M. (2006) *Cell Metab.* **4,** 61–73
42. Prusty, D., Park, B. H., Davis, K. E., and Farmer, S. R. (2002) *J. Biol. Chem.* **277,** 46226–46232
43. Orlicky, D. J., DeGregori, J., and Schaack, J. (2001) *J. Lipid Res.* **42,** 910–915
44. Orlicky, D. J., and Schaack, J. (2001) *J. Lipid Res.* **42,** 460–466
45. Ross, S. A., Song, X., Burney, M. W., Kasai, Y., and Orlicky, D. J. (2003) *Biochem. Biophys. Res. Commun.* **302,** 354–358

0013-7227/07/$15.00/0
Printed in U.S.A.

Endocrinology 148(3):1218–1225

doi: 10.1210/en.2006-0706

Undernutrition *in Utero* Augments Systolic Blood Pressure and Cardiac Remodeling in Adult Mouse Offspring: Possible Involvement of Local Cardiac Angiotensin System in Developmental Origins of Cardiovascular Disease

Makoto Kawamura, Hiroaki Itoh, Shigeo Yura, Haruta Mogami, Shin-Ichi Suga, Hisashi Makino, Yoshihiro Miyamoto, Yasunao Yoshimasa, Norimasa Sagawa, and Shingo Fujii

Department of Gynecology and Obstetrics (M.K., H.I., S.Y., H.Mo., S.F.), Kyoto University Graduate School of Medicine, Kyoto 606-8507, Japan; Departments of Etiology and Pathology (S.-I.S.) and Atherosclerosis and Diabetes (H.Ma., Y.M., Y.Y.), National Cardiovascular Center, Suita, Osaka 565-8565, Japan; Department of Obstetrics and Gynecology (N.S.), Mie University Graduate School of Medicine, Tsu, Mie 514-8507, Japan; and Precursory Research for Embryonic Science and Technology (PRESTO) (S.Y.), Japan Science and Technology Agency (JST), Kawaguchi City, Saitama 332-0012, Japan

Evidence has emerged that undernutrition *in utero* is a risk factor for cardiovascular disorders in adulthood, along with genetic and environmental factors. Recently, the local expression of angiotensinogen and related bioactive substances has been demonstrated to play a pivotal role in cardiac remodeling, *i.e.* fibrosis and hypertrophy. The aim of the present study was to clarify the possible involvement of the local cardiac angiotensin system in fetal undernutrition-induced cardiovascular disorders. We developed a mouse model of undernutrition *in utero* by maternal food restriction, in which offspring (UN offspring) showed an increase in systolic blood pressure (8 wk of age, $P < 0.05$; and 16 wk, $P < 0.01$), perivascular fibrosis of the coronary artery (16 wk, $P < 0.05$) and cardiac cardiomegaly (16 wk, $P < 0.01$), and cardiomyocyte enlargement, concomitant with a significant augmentation of angiotensinogen ($P < 0.05$) and endothelin-1 ($P < 0.01$) mRNA expression and a tendency to increase in immunostaining for both angiotensin II and endothelin-1 in the left ventricles (16 wk). These findings suggest that fetal undernutrition activated the local cardiac angiotensin system-associated bioactive substances, which contributed, at least partly, to the development of cardiac remodeling in later life, in concert with the effects of increase in blood pressure. (*Endocrinology* 148: 1218–1225, 2007)

IN THE EARLY 1990s, a novel hypothesis was advanced by Barker *et al.* (1) to link nutritional insults during embryonic and fetal periods not only to impaired maturation of physiological functions, but also to cardiovascular diseases in adulthood. Alterations in nutrition and endocrine status during the embryonic, fetal, and neonatal periods can trigger developmental predictive adaptive responses (2), causing permanent structural, physiological, and metabolic changes, thereby predisposing an individual to cardiovascular, metabolic, and endocrine diseases in adult life.

The renin-angiotensin system (RAS) plays an important role in primary as well as secondary forms of hypertension in both animals and humans (3). More recently, components of the RAS, such as angiotensin-converting enzyme (ACE) and angiotensin II, were revealed to be produced locally in the cardiac tissues, and termed the local cardiac RAS (4), being primary candidates for the factors promoting cardiac remodeling, mainly cardiac myocyte hypertrophy and increased extracellular matrix fibrosis, thereby deteriorating cardiac function (5). Various experimental animal models have been developed to investigate the associations between fetal undernutrition and cardiovascular disease later in life (6, 7), and a possible commitment of a systemic RAS in the developmental origins of hypertension was reported (8). Therefore, the aim of the present study was to investigate whether the local cardiac RAS is associated with the developmental origins of cardiac remodeling in offspring exposed to undernutrition *in utero*.

Recently, we developed a mouse model of undernutrition *in utero* using maternal food restriction, in which the offspring (UN offspring) developed pronounced obesity when fed a high-fat diet, accompanied by impaired hypothalamic leptin sensitivity, as compared with normally nourished offspring (NN offspring) (9). Using this model, we investigated whether fetal undernutrition affects systolic blood pressure (SBP), cardiac remodeling, and expression of local cardiac RAS-associated bioactive substances. We found that undernutrition *in utero* caused a significant increase in SBP as well

First Published Online November 30, 2006

Abbreviations: ACE, Angiotensin-converting enzyme; Ang, angiotensinogen; ANP, atrial natriuretic peptide; ARC, arcuate nucleus of the hypothalamus; AT1R, angiotensin II type 1 receptor; AT2R, angiotensin II type 2 receptor; BNP, brain natriuretic peptide; dpc, d postcoitum; ET-1, endothelin-1; GAPDH, glyceraldehyde-3-phosphate dehydrogenase; NN offspring, normally nourished offspring; NOx, nitrite/nitrate; PAS, periodic-acid Schiff; RAS, renin-angiotensin system; SBP, systolic blood pressure; UN offspring, offspring of undernutrition *in utero*.

***Endocrinology* is published monthly by The Endocrine Society (http://www.endo-society.org), the foremost professional society serving the endocrine community.**

as cardiac remodeling, concomitant with a significant elevation in mRNA expression in angiotensinogen (Ang) and endothelin-1 (ET-1) in the left ventricle.

Materials and Methods

Development of a mouse model of undernutrition in utero

Undernutrition *in utero* by maternal food restriction was carried out as described previously (9). In brief, pregnant C57Bl/6 mice were purchased at 8.5 d postcoitum (dpc) from Japan Central Laboratories for Experimental Animals (Tokyo, Japan) and were divided into two groups at 10.5 dpc. Dams were housed individually with free access to water during 14-h light, 10-h dark cycles. The daily food supply of one group was restricted to 70% of the food consumed by the other group, fed *ad libitum*, based on the data of the previous day, from 10.5 dpc to the day of delivery of the pups. Dams of the food restriction group were supplied 2.5 g of extra food in the evening of 18.5 dpc, just before the night of parturition, to prevent mothers from eating their own pups. Pups were nursed by mothers fed *ad libitum* (eight pups per mother) and were weaned on to regular chow diet (RCD; Oriental Yeast Co., Tokyo, Japan) at 21.5 d of age. RCD includes 20.8% protein and 4.8% fat, with contents of sodium (0.19 g/100 g) and potassium (0.75 g/100 g). Only male pups were used for the following experiments, except for the study of fetal heart tissues. Each group in all experiments consists of offspring from at least four litters. All experimental procedures were approved by the Animal Research Committee, Kyoto University Graduate School of Medicine (Med Kyo 64116).

Measurement of SBP

At 4, 8, and 16 wk of age, SBP was measured at least five times in conscious mice (n = 8–10 for each group) using an indirect tail-cuff method (MK-2000; Muromachi Kikai Co. Ltd., Tokyo, Japan).

Neonatal leptin or monosodium glutamate treatment

Leptin (2.5 μg/g body weight·d) (PeproTech Inc., Rocky Hill, NJ) or vehicle saline was sc administered to NN offspring daily from 5.5 to 10.5 d of age, as a model of premature leptin surge (9), then SBP was measured at 8 wk. Monosodium glutamate (2 mg/g body weight·d) was sc administered to NN and UN offspring from 1.5 to 5.5 d of age, as previously described (9), for the purpose of permanent chemical injury of the arcuate nucleus of the hypothalamus (ARC) (10), then SBP was measured at 16 wk.

Morphological analysis of the kidney

For morphological analysis, whole kidneys were sampled at 8 and 16 wk, weighed and fixed in 10% formalin, and embedded in paraffin. The kidneys were cut into sections 2-μm thick and stained with hematoxylin and eosin, periodic-acid Schiff (PAS), or Masson trichrome. The stained sections were analyzed light microscopically.

Serum nitrite/nitrate (NOx) and plasma angiotensin II concentration

NOx concentration was determined by the Griess reaction using a commercial colorimetric assay kit (Cayman Chemical, Ann Arbor, MI).

The angiotensin II concentration was determined with an ELISA kit (Peninsula Laboratories, Belmont, CA), after extraction through C_{18} Sep-Pak columns (Waters Co., Milford, MA).

Urine microalbumin concentration

Urine was collected for 24 h using metabolic cages, and microalbuminuria was determined by the competitive ELISA method (Albuwell M assay kit; Exocell, Philadelphia, PA) at 16 wk of age. Urine creatinine values were assessed simultaneously by enzyme assay (MIZUHO MEDY Co., Ltd., Saga, Japan) and were used to calculate the albumin to creatinine ratio.

Morphometric analysis of the heart

The whole hearts were sampled, fixed in 10% formalin, and embedded in paraffin at 8 and 16 wk. The heart was cut into two subserial cross-sections 6-μm thick at intervals of 1 mm and stained with Sirius Red to evaluate the perivascular fibrosis of coronary arteries 100–200 μm in diameter. The perivascular fibrosis was assessed by analyses of digital images, calculating the ratio of the area of Sirius Red-stained fibrosis to the total vessel area using a KS400 image system (Zeiss, Oberkochen, Germany). To evaluate perivascular fibrosis in renal small arteries 100–200 μm in diameter, the kidneys were also sampled in the offspring at 16 wk and evaluated in the same manner as the coronary arteries.

To determine the interstitial fibrosis of the heart at 16 wk of age, we randomly selected 20 fields in two different sections and calculated the ratio of the areas of Sirius Red-stained interstitial fibrosis to the total cross-sectional areas.

Cardiomegaly was assessed by whole-heart weight to body weight ratio at 8 and 16 wk. Cardiomyocyte enlargement was estimated by measuring shortest transverse diameter in nucleated transverse sections of the myocytes. In each sample at 16 wk, 8 fields were randomly selected, and 80 cells were measured.

Quantitative RT-PCR analysis

Total RNA was extracted from whole hearts of fetal mice at 18.5 dpc and from left ventricles of the mice at 3, 8, and 16 wk, as well as from kidneys at 16 wk. The mRNA expression was measured by real-time quantitative RT-PCR using Taqman technology (Model 7000 sequence detector; Applied Biosystems, Foster City, CA). The forward and reverse primers and Fam/Tamra or Fam/MGB probes used for the targeted amplification of part of the cDNAs of murine Ang, angiotensin II type 1 receptor (AT1R), angiotensin II type 2 receptor (AT2R), ACE, renin, ET-1, atrial natriuretic peptide (ANP), and brain natriuretic peptide (BNP) are summarized in Table 1. The forward and reverse primers and Joe/Tamra probes for the murine glyceraldehyde-3-phosphate dehydrogenase (GAPDH) and ribosomal RNA coding region were purchased from Applied Biosystems. Serial dilutions of total RNA sample, isolated from mouse left ventricles or kidneys, were used to construct the standard curve for each substance. The standard curves were calculated by linear regression analysis, and threshold cycle values were used to read off relative RNA amounts. An mRNA expression value was then obtained by dividing the value for the gene of interest by the value for the ribosomal RNA or GAPDH.

At first, we assessed expression of ribosomal RNA and GAPDH mRNA based on total RNA concentration assessed by optic densitometry. The fetal undernutrition significantly decreased ribosomal RNA expression, but not GAPDH mRNA expression, in the fetal heart (data not shown). By contrast, fetal undernutrition significantly decreased GAPDH mRNA expression, but not ribosomal RNA expression, in the left ventricle after birth (data not shown). Therefore, we used GAPDH and ribosomal RNA data for analyses in the fetal heart (18.5 dpc) and in the left ventricle after birth (3, 8, and 16 wk), respectively, to compensate the variation. Because fetal undernutrition did not change GAPDH mRNA expression in the adult kidney (data not shown), GAPDH data were used for analyses in the adult kidney.

Immunohistochemistry of angiotensin II, ET-1, and renin

Six-micrometer-thick sections of the paraffin-embedded whole heart were incubated for overnight at 4 C with rabbit antiserum against angiotensin-II (1:500) (T-4007; Peninsula Laboratories), ET-1 (1:500) (T-4050; Peninsula Laboratories), or goat antiserum against renin (1:1600) (kindly donated by Professor Tadashi Inagami, Vanderbilt University School of Medicine, Nashville, TN) (11). Normal goat or rabbit serum (Dako Co., Carpinteria, CA) was used as negative controls. Staining was detected using an avidin-biotin-peroxidase method kit (ELITE ABC; Vector Laboratories, Burlingame, CA) with 3,3′-diaminobenzidine as previously described (12).

Statistical analysis

Values were expressed as means ± SEM. The significance of differences was assessed with Student's *t* test. P values < 0.05 were regarded as significant.

TABLE 1. Forward/reverse primers and FAM/Tamra or FAM/MGB probes used in the quantitive PCR analysis

	Primers (5′–3′)
Ang	
Forward	CAGCACCCTACTTTTCAACACCTA
Reverse	TGTTGTCCACCCAGAATTCATG
FAM/MGB probe	TCCAAGGAACGATGAGAG
ACE	
Forward	AATCGGCCTACTGGACCATGT
Reverse	GGCCATCTTTAGCAGGTAATTGAT
FAM/MGB probe	ACCAATGACATAGAGAGTG
AT1R	
Forward	GATCGCTACCTGGCCATTGT
Reverse	GTGACTTTGGCCACCAGCAT
FAM/MGB probe	CCGATGAAGTCTCGC
AT2R	
Forward	TGCTGGGATTGCCTTAATGAA
Reverse	TCAGGACTTGGTCACGGGTAAT
FAM/MGB probe	AGCAACGTGTTACTTTG
Renin	
Forward	CACTACGGATCAGGGAGAGTCAA
Reverse	CAGCTCGGTGACCTCTCCAA
FAM/MGB probe	CAGGACTCGGTGACTGT
ET-1	
Forward	CTTCTGCCACCTGGACATCAT
Reverse	TGGTGAGCGCACTGACATCTA
FAM/MGB probe	AGCGCGTCGTACCGTA
ANP	
Forward	GCCATATTGGAGCAAATCCT
Reverse	GCAGGTTCTTGAAATCCATCA
FAM/Tamra probe	TGTACAGTGCGGTGTCCAACACAGAT
BNP	
Forward	CCAGTCTCCAGAGCAATTCAA
Reverse	GCCATTTCCTCCGACTTTT
FAM/Tamra probe	TGCAGAAGCTGCTGGAGCTGATAAGA

Ang, GenBank accession no. BC019496; Strausberg *et al.*, 2002. ACE, BC083109; Strausberg *et al.*, 2002. AT1R, BC036175; Strausberg *et al.*, 2002. AT2R, AK086334; Carninci *et al.*, 1999. Renin, NM_031192; Wilson *et al.*, 1977. ET-1, BC029547; Strausberg *et al.*, 2002. ANP, D70837; Tamura *et al.*, 1996. BNP, D82049; Ogawa *et al.*, 1994.

Results

SBP at 4, 8, and 16 wk

There was no significant difference in SBP between UN and NN offspring at 4 wk. However, the SBP of UN offspring was significantly higher than that of NN offspring at 8 wk ($P < 0.05$), and the elevation of SBP in UN offspring continued at least until 16 wk ($P < 0.01$) (Fig. 1A).

SBP after neonatal leptin or monosodium glutamate treatment

There was no significant difference in SBP between NN offspring with neonatal leptin treatment (90.5 ± 1.4 mm Hg, n = 10) and those with neonatal vehicle treatment (86.3 ± 1.6 mm Hg, n = 10) at 8 wk. The significant elevation of SBP in UN offspring, as compared with NN offspring, at 16 wk was not blocked by chemical injury of the ARC by neonatal monosodium glutamate treatment (108.1 ± 5.2 mm Hg, n = 9 *vs.* 88.8 ± 5.0 mm Hg, n = 8; $P < 0.05$).

Serum NOx concentration and plasma angiotensin II concentration

The serum NOx concentration of UN offspring was significantly lower than that of NN offspring at 8 wk ($P < 0.05$) (Table 2). Such a tendency was also observed at 16 wk, but the difference was not statistically significant (Table 2).

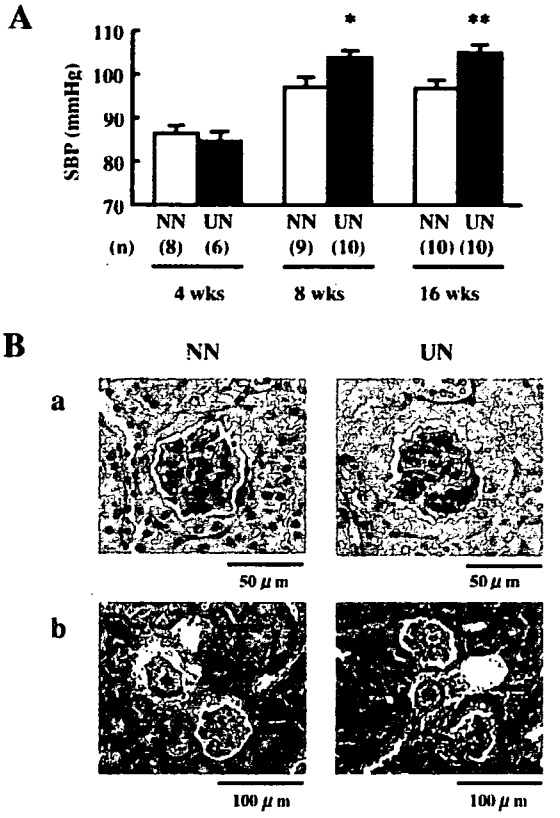

FIG. 1. SBP (A), PAS (Ba), and Masson trichrome (Bb) staining of kidney in NN offspring and UN offspring. *Columns* and *error bars* represent the mean and SEM of SBP. *, $P < 0.05$; **, $P < 0.01$ *vs.* NN offspring. Original magnification was ×400 (Ba) or ×200 (Bb). wks, Weeks of age.

The plasma angiotensin II concentration of UN offspring was similar to that of NN offspring at 8 wk (Table 2). At 16 wk, the plasma angiotensin II concentration of UN offspring was higher than that of NN offspring, but the difference was not significant (Table 2).

Urine microalbuminuria

There was no significant difference in urine microalbumin concentration between UN and NN offspring at 16 wk (25.03 ± 2.06 μg/mg creatinine, n = 7 *vs.* 22.52 ± 1.65 μg/mg creatinine, n = 8).

Morphological analysis of the kidney

At 16 wk of age, the ratio of renal weight to body weight (mg/g) in UN offspring (5.58 ± 0.32, n = 20) was similar to that of in NN offspring (5.69 ± 0.27, n = 20).

Microscopic observation of hematoxylin and eosin (data not shown), PAS (Fig. 1Ba), and Masson trichrome (Fig. 1Bb) staining of kidneys from UN offspring at 8 and 16 wk showed no histological abnormalities as compared with NN offspring including nephron numbers.

TABLE 2. Serum NOx concentrations and plasma angiotensin II concentrations

	8 wk		16 wk	
	NN	UN	NN	UN
NOx (μM)	29.1 ± 3.1 (n = 9)	19.0 ± 2.5[a] (n = 10)	19.0 ± 2.8 (n = 10)	14.2 ± 2.2 (n = 10)
Angiotensin II (pg/ml)	43.3 ± 3.5 (n = 14)	43.4 ± 4.9 (n = 11)	118.9 ± 14.0 (n = 8)	179.1 ± 38.7 (n = 8)

Values are the mean ± SEM.
[a] $P < 0.05$ *vs.* NN.

Perivascular fibrosis of the coronary artery and renal small artery

At 8 wk of age, the ratio of coronary perivascular fibrosis to total vessel area in UN offspring had tended to increase as compared with that in NN offspring; however, the difference was not significant (Fig. 2B). At 16 wk of age, the ratio of coronary perivascular fibrosis to total vessel area was significantly higher in the UN offspring than NN offspring ($P < 0.05$) (Fig. 2, A and B). By contrast, the ratio of perivascular fibrosis to total vessel area in renal small arteries of UN offspring was similar to that in NN offspring at 16 wk of age (Fig. 2C).

Interstitial fibrosis of the heart

Interstitial fibrosis of the heart in UN offspring at 16 wk was similar to that in NN offspring (Table 3A).

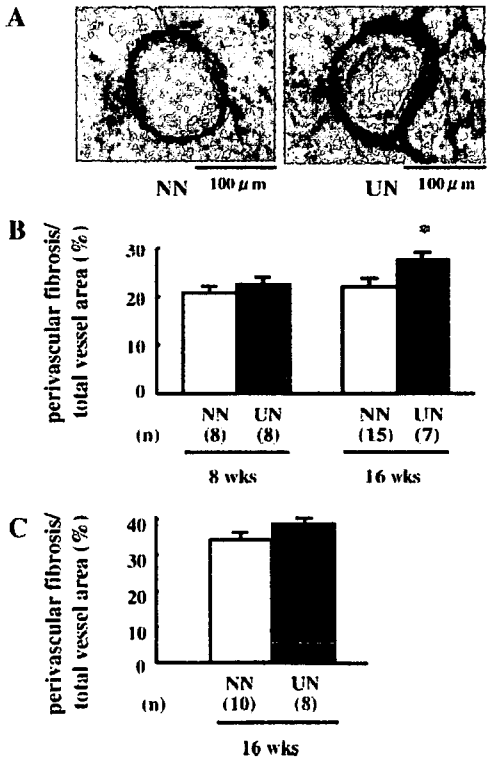

FIG. 2. Perivascular fibrosis in coronary and renal small arteries of NN and UN offspring. Representative cross-sections of coronary perivascular fibrosis at 16 wk of age (A). Collagen fibril was stained red with Sirius Red stain. Original magnification was ×400. Digital image analysis of perivascular fibrosis of coronary (B) and renal small arteries (C) as described in *Materials and Methods*. *Columns* and *error bars* represent the mean and SEM of the ratio of the area of Sirius Red-stained fibrosis to total vessel area (%). *, $P < 0.05$ *vs.* NN offspring. wks, Weeks of age.

Cardiomegaly and cardiomyocyte enlargement

The ratio of heart weight to body weight and transverse diameter of the cardiomyocytes were significantly higher in the UN offspring than NN offspring at 16 wk ($P < 0.01$) (Table 3B), in parallel with the increased perivascular fibrosis of coronary artery (Fig. 2B). However, cardiomegaly was not detected in UN offspring at 8 wk (Table 3B).

The mRNA expression of local cardiac RAS-associated bioactive substances in the left ventricles at 3, 8, and 16 wk

There were no significant changes in Ang, ACE, AT1R, AT2R, ET-1, ANP, or BNP mRNA expression between NN and UN offspring at 3 wk (Figs. 3 and 4).

At 8 wk, a significant decrease was observed in Ang mRNA expression in UN offspring ($P < 0.01$) (Fig. 3). By contrast, a significant increase was detected in AT2R ($P < 0.01$), ET-1 ($P < 0.01$), and BNP ($P < 0.01$) (Figs. 3 and 4) at 8 wk; whereas ANP mRNA expression had a tendency to increase, but not significantly (Fig. 4).

At 16 wk, a significant increase was observed in the mRNA expression of Ang ($P < 0.05$), AT2R ($P < 0.05$), and ET-1 ($P < 0.01$), but not in that of other substances (Figs. 3 and 4).

The renin mRNA expression in the left ventricles at 3, 8, and 16 wk was less than detection sensitivity of quantitative RT-PCR analysis (<0.00024-fold, compared with the whole kidney as a positive control).

Immunohistochemistry of angiotensin II, ET-1, and renin in the left ventricle

Immunostaining of both angiotensin II and ET-1 were mainly observed in cardiomyocytes of the left ventricle at 16 wk (Fig. 5, A and B). There occurred a tendency to increase in immunostaining for angiotensin II as well as ET-1 in UN offspring, as compared with NN offspring (Fig. 5, A and B).

Immunohistochemistry detected a few renin positive cells (one to two cells per slide) in the perivascular interstitial area (Fig. 5C). There was no apparent difference in the renin staining between NN and UN offspring at 16 wk (Fig. 5C).

The mRNA expression of local cardiac RAS-associated bioactive substances in the whole fetal heart at 18.5 dpc

A significant increase was observed in the mRNA expression of Ang ($P < 0.05$), ACE ($P < 0.01$), and ET-1 ($P < 0.05$) in the whole fetal heart at 18.5 dpc, but not in that of other substances (Table 4).

Discussion

In the present study, maternal food restriction caused a significant increase in SBP. However, neither the plasma

TABLE 3. Interstitial fibrosis of the heart (A) and cardiomegaly and cardiomyocyte enlargement (B)

	8 wk		16 wk	
	NN	UN	NN	UN
A. Interstitial fibrosis of the heart (%)[a]			0.782 ± 0.041 (n = 15)	0.751 ± 0.065 (n = 7)
B. Cardiomegaly and cardiomyocyte enlargement				
HW (mg)	127.1 ± 3.8	120.0 ± 3.0	158.9 ± 5.6	177.3 ± 6.2[b]
BW (g)	23.9 ± 0.2	23.2 ± 0.3	31.4 ± 0.5	30.6 ± 0.5
HW/BW (mg/g)	5.31 ± 0.13 (n = 24)	5.20 ± 0.14 (n = 19)	5.05 ± 0.12 (n = 14)	5.79 ± 0.18[c] (n = 16)
Cardiomyocyte diameter (μm)			14.3 ± 0.3 (n = 10)	16.6 ± 0.3[c] (n = 10)

Values are the mean ± SEM. HW, Heart weight; BW, body weight.
[a] No significant difference.
[b] $P < 0.05$ *vs.* NN.
[c] $P < 0.01$ *vs.* NN.

angiotensin II concentration (Table 2) nor the microalbumin concentration in UN offspring produced significant changes, although basal plasma angiotensin II concentration at 16 wk was higher than other reports (13). A significant decrease in the plasma NOx concentration of UN offspring was observed at 8 wk, as compared with that of NN offspring (Table 2). The decrease in the plasma NOx concentration of UN offspring was also observed at 16 wk, although it was not significant (Table 2). These observations suggested a possible involvement of endothelial dysfunction in the elevation of blood pressure in UN offspring, which is relevant to previous reports (14, 15). Histological examinations detected no abnormal findings in the renal tissues of UN offspring at 8 and 16 wk, although some investigators have demonstrated a possible involvement of small nephron numbers and/or a small number and size of glomeruli in increases in blood pressure during adulthood (16, 17).

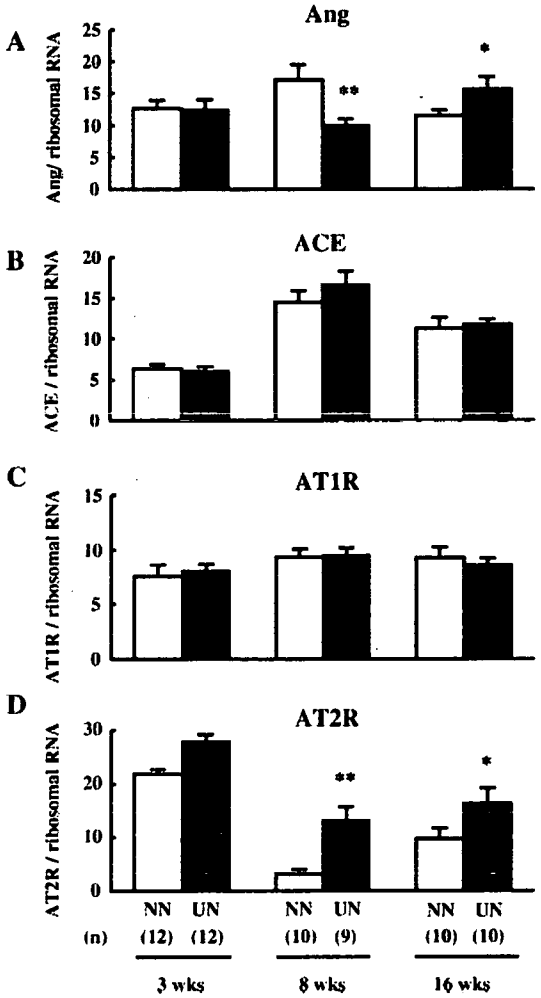

FIG. 3. The mRNA expression of Ang (A), ACE (B), AT1R (C), and AT2R (D) in the murine left ventricle at 3, 8, and 16 wk. *Columns* and *error bars* represent the mean and SEM of the mRNA expression in NN and UN offspring, measured by quantitative RT-PCR with real time TaqMan technology as described in *Materials and Methods*. *, $P < 0.01$; **, $P < 0.05$ *vs.* NN offspring. wks, Weeks of age.

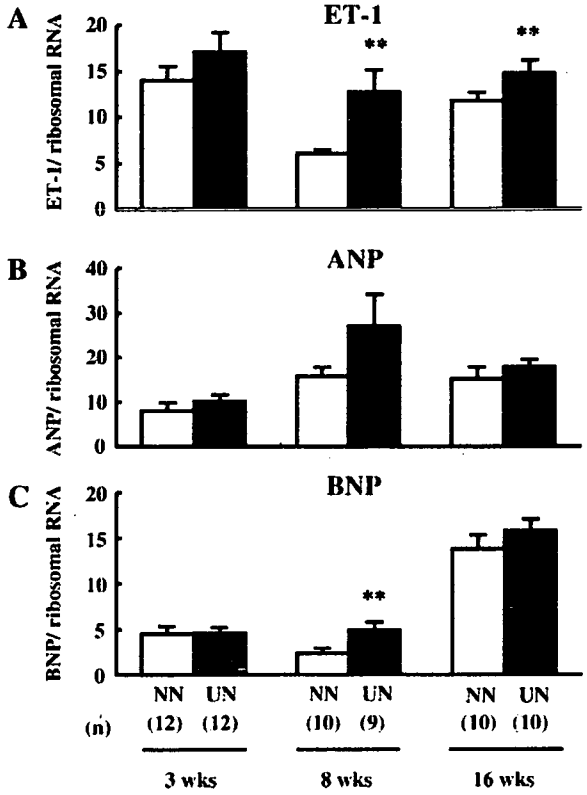

FIG. 4. The mRNA expression of ET-1 (A), ANP (B), and BNP (C) in the murine left ventricle at 3, 8, and 16 wk. *Columns* and *error bars* represent the mean and SEM of the mRNA expression in NN and UN offspring measured by quantitative RT-PCR with real time TaqMan technology as described in *Materials and Methods*. **, $P < 0.01$ *vs.* NN offspring. wks, Weeks of age.